

TESTING AND COMMISSIONING BUILDING CONTROLS THROUGH
CO-SIMULATION VIA ENERGY MODELING AND THE BUILDING CONTROLS
VIRTUAL TESTBED

A Thesis

Presented in Partial Fulfilment of the Requirements for the

Degree of Master of Science

with a

Major in Mechanical Engineering

in the

College of Graduate Studies

University of Idaho

by

Tyler Noble

Major Professors: Ralph Budwig, Ph.D., P.E., and Kevin Van Den Wymelenberg, Ph.D.

Committee Members: John Gardner, Ph.D., P.E.

Department Administrator: Steven Beyerlein, Ph.D.

July 2016

AUTHORIZATION TO SUBMIT THESIS

This thesis of Tyler Noble, submitted for the degree of Master of Science with a major in Mechanical Engineering and titled “TESTING AND COMMISSIONING BUILDING CONTROLS THROUGH CO-SIMULATION VIA ENERGY MODELING AND THE BUILDING CONTROLS VIRTUAL TESTBED,” has been reviewed in final form.

Permission, as indicated by the signatures and dates given below, is now granted to submit final copies to the College of Graduate Studies for approval.

Major Professor: _____ Date _____
Ralph Budwig, Ph.D., P.E.

Major Professor: _____ Date _____
Kevin Van Den Wymelenberg, Ph.D.

Committee
Members: _____ Date _____
John Gardner, Ph.D., P.E.

Department
Administrator: _____ Date _____
Steven Beyerlein, Ph.D.

ABSTRACT

Computer energy models were developed for controller-in-the loop co-simulation using the EnergyPlus software and the Building Controls Virtual Testbed. Models were constructed to approximate building envelopes and mechanical systems. The models simulated inputs expected by building controllers and desired output signals were communicated back into EnergyPlus at set simulation time increments. This research extends previous work which demonstrated control of economizing function of an air handling unit by investigating control of additional functions including supply air temperature control. By adjusting the supply air temperature modulation range according to techniques described in this paper it is estimated that up to 124 MWh (7%) savings in total facility energy would be realized. Additional research was performed into virtual control of multiple air handling units and multiple controllers-in-the-loop. The challenge of programming controllers for constant air volume units with no zone reheat terminals is examined. Reduction of hours of unmet heating setpoint during occupied times as well as effects on system energy usage are realized. Effects of adjusting system performance towards minimizing unmet hours may result in up to a 30% increase in energy use. Suitability of energy modeling and co-simulation for pre-commissioning building automation and control systems is discussed.

ACKNOWLEDGEMENTS

I would like to thank Ralph Budwig for being an exceptional mentor during my time as a graduate student and offering substantial advice and guidance in developing this thesis; Kevin Van Den Wymelenberg for his advice regarding this research especially as it relates to introducing this research topic and offering research suggestions; Committee member John Gardner for his service including efforts to read and evaluate this work; Elizabeth Cooper for her support of this work and for providing opportunities to work on related projects at the Integrated Design Lab; Avista Utility Group and Idaho Power for their financial support for this and other research I participated in as a graduate student; University of Idaho facilities management personnel including Chuck Schoeffler, Kristyn Hardy, and Benjamin Camp for their generous assistance in gathering critical information for the energy models as well Alerton equipment used in this study; Damon Woods for sharing much expertise in energy modeling and providing collaborative support for this work; Brad Acker, for his expertise and participation in the Avista sponsored BCVTB research related to the College of Business and Economics Building; Sean Rocke of Control Sentries of Idaho for donating time and lending equipment for use in this research; and ATS Inland NW for providing support and information on the Alerton equipment.

DEDICATION

To my loving wife Rylee and our sweet daughters Ameilya and Madilynn.

Thank you for your support.

TABLE OF CONTENTS

AUTHORIZATION TO SUBMIT THESIS	ii
ABSTRACT	iii
ACKNOWLEDGEMENTS	iv
DEDICATION	v
TABLE OF CONTENTS	vi
LIST OF TABLES	viii
LIST OF FIGURES	x
1 PREFACE	1
2 OPTIMIZATION OF SUPPLY AIR TEMPERATURE USING CONTROLLER- IN-THE-LOOP CO-SIMULATION	2
2.1 Abstract	2
2.2 Introduction	2
2.3 Materials and methods.....	8
2.3.1 Model facility.....	8
2.3.2 Model HVAC system	8
2.3.3 Energy model	9
2.3.4 BCVTB model.....	10
2.3.5 Alerton controller	12
2.3.6 Controller affect on co-simulation execution	17
2.4 Results and discussion	18
2.4.1 T_{SA} modulation in Case X and underlying signals	18

2.4.2	Comparison of T_{SA} response, Case Y versus Case X.....	22
2.4.3	Energy end use comparison	22
2.5	Conclusion.....	25
3	DYNAMIC PROGRAMMING AND VIRTUAL COMMISSIONING OF BUILDING CONTROL SYSTEMS THROUGH CO-SIMULATION.....	27
3.1	Abstract	27
3.2	Introduction	27
3.3	Case study background	30
3.3.1	HVAC system	31
3.3.2	Controllers	32
3.4	Materials and methods.....	34
3.4.1	Energy model	34
3.4.2	BCVTB model.....	45
3.4.3	Programming of key variables	48
3.5	Results	59
3.5.1	SAT control in heating mode for January cases	59
3.5.2	Economizer control in august cases	68
3.6	Discussion	75
3.6.1	January cases.....	75
3.6.2	August cases.....	77
3.7	Conclusion.....	78
4	SUMMARY AND CONCLUSIONS.....	81
	REFERENCES	85

LIST OF TABLES

2.1	Comparison of AHU supply fan airflow contrasting the two existing units maximum flow rate.	9
2.2	List of controller input and output signals. Economizer input AV-10 is generated as an output from the SAT loop. Thus economizer logic is partly dependent upon SAT control loop. AV-10 is an output from the SAT loop and is re-used in the economizing loop.	13
2.3	List of sample EnergyPlus zones used to monitor occupancy and draw cooling and heating signals for use with BACS controller. Location and floor area information is indicated.	17
2.4	Comparison of total facility energy simulated for cases Y and X.	23
2.5	Percent change in energy end uses. Reductions shown from Case Y to X, Parentheses indicate (Increases).	23
3.1	Comparison of AHU supply fan airflow contrasting actual air balance data with facility design and modeled values for five AHUs.	31
3.2	List of items controlled in facility BACs network along with the respective device information.	32
3.3	List of Alerton BACnet controllers used in co-simulations with respective AHUs.	32
3.4	Settings for OAT reset setpoint manager for selected cases. Temperatures listed are in °C.	40
3.5	Comparison of PI and scaling parameters selected for AHU-3 only for iterative sub-cases B-1.1 through B-1.4. Units of temperature are °C.	53
3.6	Comparison of PI and scaling parameters selected for all AHUs for case B-1. Units of temperature are °C.	54
3.7	Comparison of PI and scaling parameters selected for all AHUs for case B-2. Units of temperature are °C.	54

3.8	List of changes made between cases A-1 and A-4 to control economizer damper modulation. “NR” used to indicate that a particular parameter is not required in the logic.	57
3.9	Full description of key temperatures indicated as abbreviated temperature symbols used in Table 3.8. Identical symbols used in subsequent sections have the same meaning.	58
3.10	Full names referenced to abbreviated temperature symbols used in Figure 3.15. Identical symbols used in subsequent figures have the same meaning.	60
3.11	Comparison of (t_{HSPX}) hrs. during occupied times for each control (CZ) and (SZ) for cases B-1 and B-2 during January. Temperature units are in °C.	62
3.12	Time heating setpoint is not met, (t_{HSPX}) in (hrs.), during occupied times for the five control zones for cases B-1.1 through B-1.4 as well as results from B-2 for Jan. 22-24.	63
3.13	Comparison of cooling energy use (kWh) for cases A-1 through A-4 for the month of August	74

LIST OF FIGURES

2.1	Energy model calibration comparison contrasting actual 2014 electrical energy with modeled electrical energy for each month throughout an annual simulation.	10
2.2	Diagram of control network used in co-simulation [28].	12
2.3	Illustration of communication of expected controller inputs indicated in Table 2.2 as required for desired output T_{SASP} (AV-19).	13
2.4	AHU key control parameters including supply air temperature (T_{SA}), return air temperature (T_{RA}), mixed air temperature (T_{MA}) and outside air temperature (T_{OA}).	14
2.5	Snapshot of AHU-1 SAT control loop showing required signals for generation of a SAT SP.	15
2.6	Snapshot of AHU-1 SAT control loop showing required signals for generation of the ACP signal.	16
2.7	Controller in the loop modulation of AHU supply air temperature T_{SA} for Case X for a one week period in July (Jul. 9-16). Units of temperature are °C. Relationship between \dot{Q}_{ZCE+} and T_{SA} is highlighted for a summer period showing reduction in T_{SA} where cooling load occurs. \dot{Q}_{ZCE+}	19
2.8	Controller in the loop modulation of AHU supply air temperature T_{SA} for Case X for a one week period in July (Jul. 9-16). Units of temperature are °C. Relationship between zone occupancy and T_{SA} is highlighted for a summer period showing reduction in T_{SA} where occupancy increases.	20

2.9	Controller in the loop modulation of AHU supply air temperature T_{SA} for Case X for a one week period in January (Jan. 9-16). Outside air temperature T_{OA} is also shown. Units of temperature are °C. Relationship between \dot{Q}_{ZCE+} and T_{SA} is highlighted for a winter period showing occasional reduction in T_{SA} where cooling load occurs. \dot{Q}_{ZCE+} signals are only included for two of the ten sample zones.	21
2.10	Comparison of T_{SA} response for cases Y (left) and X (right). Case Y shows constant T_{SA} response while Case X shows a modulating response.	22
2.11	Tradeoff in selected energy end uses in MWh showing reductions from Case Y to X. Results are for an annual run period. (Tradeoffs resulting in zero percent change are omitted). Values between parentheses indicate energy increases. . . .	24
2.12	Comparison of energy end use between cases X and Y.	24
3.1	Comparison of actual (left) to modeled geometry (right). Picture of actual geometry is courtesy of Google Satellite Imagery.	31
3.2	Diagram of BACnet controller network used in co-simulations showing: A.) Typical 12 GB desktop PC, B.) Netgear Ethernet hub, C.) Mach-ProWebCom MSTP to BACnet IP gateway device, D.) Alerton VLCA-1688, E.) Alerton VLC-1188, F.) Alerton VLC-1600, G.) Typical Power Supply and H.) Typical 24 V dc power supply	33
3.3	Comparison of monthly actual to modeled electrical energy use for cases Q-1 and R-1 throughout 2014.	37
3.4	Comparison of monthly actual to modeled natural gas energy use for cases Q-1 and R-1 throughout 2014.	38
3.5	Comparison of total facility energy use simulated using cases Q-1 and Q-2 throughout all of 2014.	40
3.6	Comparison of total facility energy use simulated using cases R-1 and R-2 throughout all of 2014.	41

3.7	Comparisons of energy end uses simulated using cases Q-1 and Q-2 throughout all of 2014.	42
3.8	Comparisons of energy end uses simulated using cases R-1 and R-2 throughout all of 2014.	42
3.9	Example real time simulation output plot generated by BCVTB showing AHU-2 system temperatures for case B-1.1. Time is along the axis of abscissas displayed in $(s) \cdot 10^5$. The simulation run period was January 22-24 and only data from the first two simulated days are shown. Temperature displayed along the ordinate is in $T \cdot 10^2$. Choice of temperature scale for real time co-simulation output was in $^{\circ}\text{F}$. SI units are used for duration of this paper.	49
3.10	Example real time simulation output plot generated by BCVTB showing AHU-1 economizer damper position for a typical co-simulation. Time for the entire month of June is along the axis of abscissas, displayed in $(s) \cdot 10^6$	50
3.11	Illustration of programming for control of SAT.	51
3.12	Inputs and outputs of Alerton PI block	52
3.13	2 – IN scaler block used to produce T_{SASP} along with input logic designed to produce step increase in both T_{SAH} and T_{SAL} at times when (T_{HSP}) is greater than the control zone temperature (T_{CZ})	56
3.14	View of partial screenshot showing portion of logic for SAT control as well as PI blocks used for generating heating and cooling signals.	57
3.15	AHU-2 system temperatures contrasting T_{CZ} response T_{SA} with T_{SASP} for case C-1 using Model Q and simulation run period Jan. 18-24.	60
3.16	AHU-2 system temperatures contrasting T_{CZ} response T_{SA} with T_{SASP} for case B-2 using Model R and simulation run period Jan. 18-24.	61
3.17	AHU-3 system temperatures contrasting T_{CZ} response T_{SA} with T_{SASP} for case B-1 using Model R and simulation run period Jan. 18-24.	63

3.18 AHU-3 system temperatures contrasting T_{CZ} response T_{SA} with T_{SASP} for case B-2 using Model R and simulation run period Jan. 18-24.	64
3.19 AHU-3 system temperatures contrasting T_{CZ} response with T_{HSP} for case B-1 using Model R and simulation run period Jan. 18-24.	64
3.20 AHU-3 system temperatures contrasting T_{CZ} response with T_{HSP} for case B-2 using Model R and simulation run period Jan. 18-24.	65
3.21 AHU-3 system temperatures highlighting T_{CZ} response, T_{SA} , for case B-1.1 using Model R and simulation run period Jan. 22-24.	66
3.22 width=3in	66
3.23 AHU-3 system temperatures highlighting T_{CZ} response, T_{SA} , for case B-1.3 using Model R and simulation run period Jan. 22-24.	67
3.24 AHU-3 system temperatures highlighting a well tuned T_{CZ} response, T_{SA} , for case B-1.4 using Model R and simulation run period Jan. 22-24.	67
3.25 Comparison of AHU-3 total heating energy between sub-cases B-1.1 through B-1.4.	68
3.26 Comparison of total facility energy use between cases B-1 and B-2.	69
3.27 Signals for damper open fraction for all AHUs from case A-1.	69
3.28 Signals for damper open fraction for all AHUs from case A-2.	70
3.29 Signals for damper open fraction for all AHUs from case A-4.	71
3.30 AHU-3 system temperatures for case A-1 throughout five day time period from Aug. 6-10.	72
3.31 AHU-3 system temperatures for case A-2 throughout five day time period from Aug. 6-10.	72
3.32 AHU-3 system temperatures for case A-3 throughout five day time period from Aug. 6-10.	73
3.33 AHU-3 system temperatures for case A-4 throughout five day time period from Aug. 6-10.	73

3.34 Percent change, increases and (decreases), in cooling energy use between selected cases. 75

CHAPTER 1

PREFACE

This thesis is presented as two journal papers which are organized into separate chapters, excluding references. As several citations are identical between the two papers references for both papers are combined at the end of chapter three. The papers are formatted to stand-alone and as such each includes its own abstract, introductions, methods, results, discussion, and conclusion sections.

Chapter 2, “OPTIMIZATION OF SUPPLY AIR TEMPERATURE USING CONTROLLER-IN-THE-LOOP CO-SIMULATION” is a report on preliminary studies focused on the feasibility of the Building Controls Virtual Testbed for commissioning air handler controllers. Chapter 3, “DYNAMIC PROGRAMMING AND VIRTUAL COMMISSIONING OF BUILDING CONTROL SYSTEMS THROUGH CO-SIMULATION” is a paper focused on the use of co-simulation to assist in programming and testing building controls. Real building controllers are used to virtually control variables of multiple air handling units in a co-simulation using two different model representations of a single facility. Challenges involved in programming and controlling constant volume air handling units with no zone re-heat are examined using co-simulation facilitated by the Building Controls Virtual Testbed. Both reduction of unmet heating setpoint hours during occupied times as well as effects on energy usage are examined.

The intent of these studies was to further validate tools capable of integrating energy simulation into controls commissioning. Both strengths as well as deficiencies in terms of the potential for using the Building Controls Virtual Testbed (BCVTB) as an integration tool are identified. Various likely resolvable compatibility issues with the energy modeling software used in these studies are also identified. In addition to this intent, documenting processes used to perform controls research was also of particular interest. An effort is made to provide adequate details in these reports both to provide examples of how this technique can be employed as well to stimulate ideas of how similar problems may be solved.

CHAPTER 2

OPTIMIZATION OF SUPPLY AIR TEMPERATURE USING CONTROLLER-IN-THE-LOOP CO-SIMULATION

2.1 Abstract

A co-simulation model was developed for a controller-in-the loop energy simulation using the EnergyPlus software and the Building Controls Virtual Testbed in addition to a physical building controller. The energy model simulated inputs expected by the controller and the desired output signal was communicated back to EnergyPlus at set simulated time increments. This research builds upon previous efforts using this platform to control economizer damper position and investigates developing techniques for control of additional parameters. Control of supply air temperature modulation of an air handling unit towards potential energy savings was the primary task studied and techniques are demonstrated for apparently correct control. Based on results from studies adjusting supply air temperature modulation range it is estimated that up to 124 MWh (7%) savings in total facility energy would be realized by demonstrated techniques.

2.2 Introduction

Buildings are greatly dependent on their control systems for efficient operation of connected systems. Energy efficient operation, level of occupant comfort and other environmental factors are all affected by building automation and control systems (BACSs). Controls that have not been adequately debugged or whose settings are no longer adequate for aging equipment can negatively impact performance of key building systems. Project specifications usually include provisions for commissioning of building systems and their controls. Specific benefits of commissioning automation equipment are well documented. Many benefits of these activities are discussed in [5], [3] and [11]. In [5], Harmer and Henze demonstrate use

of a calibrated energy model within an energy management application as an extension to typical capabilities of model based commissioning. Their monitoring based commissioning system which employed energy modeling techniques made successful predictions for energy and demand with respect to both magnitude and timing. The system also predicted shortfalls in cooling capacity. In [3], Dong et al. apply model-based Fault Detection Diagnostics (FDD) through a Building Information Modeling (BIM) enabled information infrastructure. The authors noted that anywhere between 5-30% savings in energy are achievable through FDD. Using their platform for FDD the authors demonstrated an efficient information exchange process that was implemented in a real building. Benefits of implementing the BIM-enabled framework for FDD are discussed in terms of potential improvements in information exchange efficiency. The research described in [3] provides support for the practice of on-going commissioning efforts. In [11], Liu et al. research alternatives to traditional methods to analyze data generated during the design process. Through a data-driven approach, the authors provide examples of how a number of computing tools may be integrated into the design process leading to subsequent improvements in the built environment.

A typical commissioning process generally begins when a building project is near completion as installing contractors finish system connections, perform start-up procedures and make adjustments to equipment and controls in an effort to bring their performance in line with design intent. Various tests are performed to ensure proper system function. This form of commissioning requires significant effort as well as time during the first months and sometimes even years of a building's functional life. It is not uncommon for this process to challenge project participants and even building occupants as issues of varying urgency are addressed. So long as apparent issues persist, the initial commissioning period drags on.

Under this more typical commissioning effort, occasionally equipment issues fall under the radar. Such issues may result in excessive operation costs, poor operational performance and even damage accumulation as time progresses. One example of a possible issue could be an incorrect rotational direction of exhaust fans resulting in poor evacuation of effluent

from cooking or other activities. A second example could be instances where incorrectly programmed or wired systems result in equipment sequence of operation incompatible with the design intent. An example of this could be a supply fan damper remaining completely shut or fan motor not even switching on for months or sometimes years of a buildings life. It is not uncommon for critical building systems such as air handling units as well as heating and chilled water plants to be found operating below planned or optimal efficiencies because of control issues [22]. Another form of commissioning includes activities performed as part of an ongoing process of system monitoring and maintenance. Thus building operators and maintenance personnel take an active role in ongoing commissioning.

Sometimes it is the unforeseen or unanticipated actual facility or environmental conditions which buildings and their equipment are subjected to which cause challenges and problems. Required system integration with unanticipated customizations or product features newly added by manufacturers of equipment which were not specifically called for in design are examples. Effects of local climate conditions and unforeseen effects on materials or equipment are other examples. Regardless of the reason for a rough transitional period, minimizing these issues is greatly desirable. The extent to which issues can be prevented or at least detected and resolved earlier in the game, will pay large dividends in terms of smooth operation and satisfied occupants. Thus applying more effective techniques even in a pre-commissioning effort within project design phases or just prior to implementation of systems is a subject receiving great attention, especially in the building automation community. Development of both processes and tools that integrate energy modeling into the design and commissioning project phases may result in substantial benefits including efficiency increases and improved equipment operation.

Several studies have focused on the topic of more advanced integration efforts. Wang et al. use energy modeling to demonstrate the process of ongoing commissioning efforts and demonstrate an actual savings of 10% after implementations of measures [22]. In [11] a data driven approach for directing the workflow of an integrated design process is explained.

Ideally advanced approaches for commissioning will focus both on a well formulated process as well as innovative tools. A structured process for simulation based support of building automation systems with a focus on both key automation tasks as well as building simulation is presented in [10]. The authors define a new service for this purpose. Further development and vetting of integration processes as well as the tools that support them is critical for improvements to building commissioning.

The BCVTB is one tool capable of integrating both energy models and building controls in a co-simulation [6] and [24]. The BCVTB has been the subject of much interest and use of it has been demonstrated for specific co-simulation tasks including modeling efforts using energy simulation software and MATLAB for controls as in [19] and [4]. The ability to connect the program to physical building controllers is demonstrated in [12] and has been available for some time, but extensive use of this tool for performing accelerated validation of control schemes using controller-in-the-loop simulations has not been demonstrated as of this writing. This form of validation can be a useful exercise as part of the project design phase or a pre-commissioning effort. The ability to predict the results of controller programs and settings on HVAC performance earlier in the project timeline would help towards achieving a smooth commissioning process. Before tools such as BCVTB and any similar solutions may be integrated into the design phase their utility must be adequately validated. Also integrating features of a BCVTB or other solution would ideally be good enough for rapid implementation and support rapid analysis of simulation results.

In [28], proof-of-concept of pre-commissioning building controllers is demonstrated using co-simulation. In this previous study a BACnet compatible controller is connected to a calibrated energy model which approximates the building envelope and HVAC system of a 4,600 m^2 three-story building. The experiment set-up used was designed to test and optimize economizer settings. The energy model was developed using both OpenStudio and EnergyPlus software and a path of communication was established between the energy model's primary air-handling unit (AHU) and the physical controller by means of the Building Controls Vir-

tual Testbed (BCVTB). Communication was established such that the signal for economizer damper position was provided to the EnergyPlus simulation by the BACnet controller in lieu of the program's default controller for economizing. Conducted simulations and reviewing their results allowed for commissioning the BACnet device completely virtually. Through virtual commissioning efforts, it was discovered that a combination of adjustments in configuration settings and economizer lock-out temperature would result in 12% (190,000 kWh) energy savings per year.

The DDC device used in the control loop in the previous study was an Alerton VLCA-1688 which is the same device by which the actual equipment is controlled. In the present study the same AHU and facility is examined for a similar commissioning effort focusing on a different feature. In this case control of the unit's supply air temperature (SAT) at the AHU discharge point is what was controlled. In addition to controlling SAT, this model also included the logic and configuration from the previous study required for using the controller derived economizing signals. The process required for establishing energy model communication with the controller which handles SAT is explained.

The vendor supplied conventions for handling modulation of SAT are studied and parameters specifying the modulation range are adjusted to determine effects on energy use using controller-in-the-loop co-simulation of a one year period. Logic identical to that used to control the primary AHU in the actual building was loaded to the controller. While gathering controller information it was determined that the SAT modulation mode set in the actual controller was for manual control to a single setpoint of 12.8° C all the time. Thus an investigation into potential effects of a modulated point are of actual interest for this facility.

Certain expected controller signal inputs had to be derived using appropriate EnergyPlus conventions which included the selection of correct output variables for these purposes. The ability of the BCVTB software to handle control logic was used to process these signals to the expected behavior and form for these particular input signals. The intent of this study is not the development of customized control algorithms or systems but rather to

expand the ability of an existing energy model to allow for modulation of its AHU SAT using a physical building controller. One key reason for performing this research was to expand the efforts of the previous study presented in [28] to include more control parameters. Optimization of a handful of controlled AHU features can have further impact on energy savings and system performance. For instance, Wang et al. predict that cost savings up to 11% may be realized by reducing cooling load through increasing the design SAT setpoint (typically 13°C.) [21]. Another reason for this additional research is that the current and previous studies were precursor efforts for more extensive investigation into the possibility of more expansive studies. An example of an expanded study into this topic would be demonstrating scalability of BCVTB implementation as a means to test multiple AHUs while using additional controllers in the loop.

Another interesting aspect of AHU control that would seem ideal for co-simulation is regulation of supply or return fan speed for controlling rate of airflow. For instance one way in which energy may be saved is through reset of minimum airflow in the system to an even lower level at times of unoccupancy. Optimizing fan speed for typical operation through modulation as well as for setback situations would have been a useful thing to include as part of this study. Through this research, however, it was discovered that EnergyPlus does not as of this writing have a convention for control of AHU fan speed using an external interface such as BCVTB. While other energy management features and conventions are provided for this purpose, use of these features was not the intent of this research. Thus investigating controller based fan speed was not possible in this study.

The remainder of this paper discusses the methods involved and approach to co-simulation of controller derived SAT setpoint as an input into the energy model. Also presented are results and insights from results between two cases. Results for an annual co-simulation modeling AHU SAT modulation handled by a BACnet controller during co-simulation are compared with results from another simulation which uses identical settings except a manual constant SAT setting is simulated. The latter case also uses idealized economizer operation

instead of controller based operation. This is an important note as idealized EnergyPlus control of economizer has been shown to indicate higher energy savings than similar BACS control in reality [28].

2.3 Materials and methods

This section first briefly discusses the facility and HVAC equipment as well as the various components making up the co-simulation model. Key details regarding the energy model and an explanation of incorporating the energy model into the BCVTB environment which enables the co-simulation are also discussed. Subsequently information related to the controller signals as they relate to the simulation results are explained.

2.3.1 Model facility

The study facility is the College of Business and Economics Building of the University of Idaho in Moscow, Idaho. This building has a conditioned floor area of 4,600 m^2 and three-stories above ground. There is also a basement level below. The building is an example of a typical office building and has a variety of classrooms and offices. At present time the facility is roughly fifteen years old, thus construction materials and methods used are modern.

2.3.2 Model HVAC system

The HVAC system consists of two large AHUs with reheat at each variable air volume air terminal at each zone. Air terminals of this type are referred to as VAV boxes throughout this paper. Each VAV box requires inputs from zone thermostats which determine whether a heating or cooling signal is required by the box.

The supply airflows indicated for each AHU in the facility's mechanical schedule documents were selected as the values used in the energy model. These values are shown in Table 2.1. As seen in Table 2.1 AHU-1 is a substantially larger unit than AHU-2 and its control,

Table 2.1: Comparison of AHU supply fan airflow contrasting the two existing units maximum flow rate.

Unit	Design airflow $\left(\frac{m^3}{s}\right)$
AHU-1	26.5
AHU-2	4.1

along with that of the reheat air terminals it serves, are largely responsible for the conditioning energy required by the facility. The equipment associated with AHU-1 serves both the main and second levels of the facility while AHU-2 only supplies conditioned air only to the basement. For these reasons, the test controller was set up to control SAT setpoint (SP) for AHU-1 as changes to its function would tend to have a greater impact on energy use.

2.3.3 Energy model

The EnergyPlus model was constructed mostly using the front end application called OpenStudio which includes a graphical interface by which a user can construct an energy model. EnergyPlus conventions for modeling VAV systems with zone reheat are convenient because they lead to proper regulation of space temperatures at the zone level during a simulation. Unlike constant air volume systems with no reheat air terminals, the system modeled has adequate controls to appropriately model energy required to maintain adequate space temperature.

Energy simulated by the model closely matches actual facility use as is shown in Figure 2.1 where the modeled electrical energy for a complete annual simulation using 2014 actual meteorological data (AMY) shows very close consistency across twelve months. This agreement is quantified using the ASHRAE 14-2002 calibration method. ASHRAE energy model calibration requires calculations for normalized mean biased error (NMBE) and coefficient of variation for root mean square error CV(RMSE). NMBE determines whether the model comprehensively over or under predicts energy usage, whereas CV(RSME) assesses how closely monthly predictions correlate to monthly utility data. The guideline specifies

that CV(RMSE) below 15% as well as NMBE of 5% or less indicates satisfactory correlation [2]. In this case calculations using this method indicated values of 5.23 and -1.83 for CV(RMSE) and NMBE respectively for case Q-1. The same calculations for R-1 yield values of 14.38 and 9.59 CV(RMSE) and NMBE respectively.

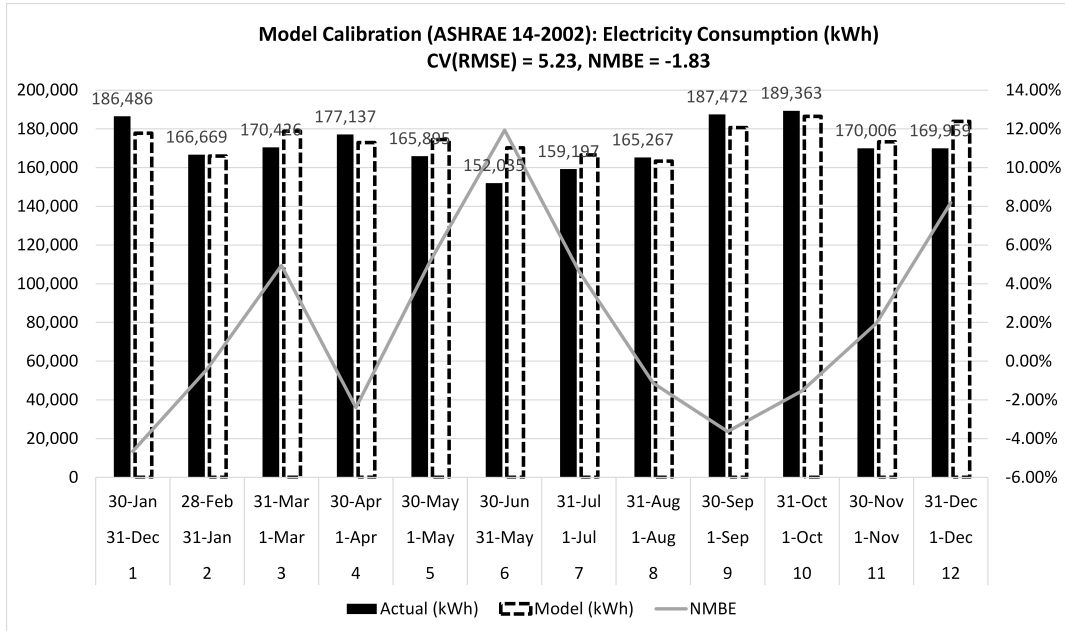


Figure 2.1: Energy model calibration comparison contrasting actual 2014 electrical energy with modeled electrical energy for each month throughout an annual simulation.

Based on review of these results it was determined that the model was a reasonable estimation of the actual facility. Thus co-simulations could be used to estimate the energy impact of modulation of AHU-1 SAT between two values. Model X which is referred to in later results represents the actual energy model with identical parameter settings compared to the co-simulation case examined in model Y which only differs in that the Alerton VLCA-1688 is used to determine AHU-1 SAT setpoints throughout the run period. These naming conventions for the two models will be used throughout the duration of this paper.

2.3.4 BCVTB model

Currently controller-in-the-loop co-simulation with any of the leading energy modeling applications requires use of a middleware software application such as BCVTB. Also BCVTB

is the only available option which supports BACnet communication within this form of co-simulation. Thus use of BCVTB was critical for this project.

The BCVTB model was designed to facilitate communication between the energy model and the BACnet controller which in this case is the Alerton VLCA-1688. Because of this, initialization of all co-simulation executions occurred within the BCVTB platform. Some initial analysis could also be performed within the application during simulations. The co-simulation model was designed to produce signal graphs of desired signals and outputs in real time. This feature is particularly useful in situations where results are obviously not desirable and would not require careful analysis as was the case with some initial attempts at SAT control. In such cases simulations may be terminated prior to completion which can save some time.

Prior to running co-simulations with the energy model, substantial development within the BCVTB platform was required. EnergyPlus input data files (.idf) were exported from OpenStudio and changes necessary to prepare the files for use with BCVTB were made using a notepad application. Connection between all variables communicated between the controller and EnergyPlus had to be manually linked graphically with BCVTB's interface. A supporting configuration file (.cfg) linking EnergyPlus variable to the external interface was also required which made connections between the software. This file included information on variable type and specified the path of communication. For communication with a BACnet devices BCVTB relies on the BACnet stack, a data communication protocol for building automation and control networks. As such additional configuration files written using extensible markup language (.xml) are required. The syntax required by these files is easy to pick up and examples of the required files are provided in the BCVTB documentation [25]. The BCVTB co-simulation model is also a required configuration file which exists as an .xml file. This file is used to execute co-simulations within BCVTB. Several other details of this process including various issues and the techniques used to resolve them are explained in [28].

2.3.5 Alerton controller

A diagram of the network setup for the Alerton VLCA-1688 used in co-simulation for this study is shown in Figure 2.2. The items included in the IP network are simply the VLCA-1688 and a typical laptop PC running on twelve gigabytes of RAM. Communication between the controller device and the PC is handled by a standard Ethernet cable.

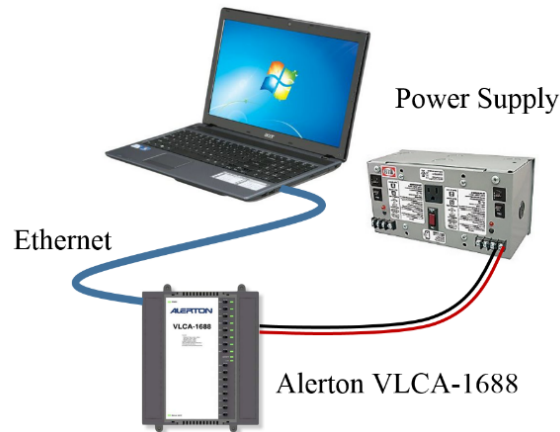


Figure 2.2: Diagram of control network used in co-simulation [28].

The controller was programmed using the front end application developed by the manufacturer called Envision for BACtalk. This program includes an extension for Microsoft Visio which allows the DDC programmer to use visual logic to design control loops and sequences. A list of all inputs and outputs required for the SAT SP control are included in Table 2.2. Each parameter is shown beside its BACnet object number. These numbers are part of the identification information required by protocol. A particular parameter must be uniquely identified by one of these numbers. All information shown in Table 2.2 was transmitted over the Ethernet connection between the controller and the computer. The input parameters shown were all necessary for function of the loop with respect to the output signals used in simulation. In this paper the output signal of interest is the SAT setpoint, T_{SASP} , which is identified in Table 2.2 as AV-19. An illustration of the full communication loop required to achieve T_{SASP} as an output signal is shown in 2.3. This setpoint is used to control the temperature of air as it discharges from the air handling unit. Control parameters of particular

Table 2.2: List of controller input and output signals. Economizer input AV-10 is generated as an output from the SAT loop. Thus economizer logic is partly dependent upon SAT control loop. AV-10 is an output from the SAT loop and is re-used in the economizing loop.

Inputs	Objects	Outputs	Objects
Freeze Stat Status	BI-8	Econo Command	AV-26
Fan Status	BI-5	Econo % Reversed for Display	AV-29
VAV's in Warmup	AV-40	Mixing Damper Command	AO-4/AV-27
OSA Temp	AV-0	OSA Damper Command	AO-3/AV-27
Econo lockout temp	AV-56	AHU-1 SAT Cooling Signal	AV-10
OSA Temp	AV-0	AHU-1 SAT setpoint	AV-19
RAT	AI-2		
Min OSA %	AV-65		
MAT	AI-1		
MAT Max Stpt	AV-60		
MAT Min Stpt	AV-61		
Cooling Signal	AV-10		
Manual SAT Stpt Mode	BV-11		
Average Cooling Percent	AV-53		
Max SAT Stpt	AV-57		
Min SAT Stpt	AV-58		
Supply Fan Status	BI-5		
Cooling Time Loop	BV-20-N		
VAV Total Heating Signal	AV-49		
VAV Total Cooling Signal	AV-51		
Total VAV's in Occupied	AV-42		
AHU-1 SAT	AI-0		
Cooling Error Divisor	AV-55		
Average Heating Signal	AV-52		
Average Cooling Signal	AV-53		

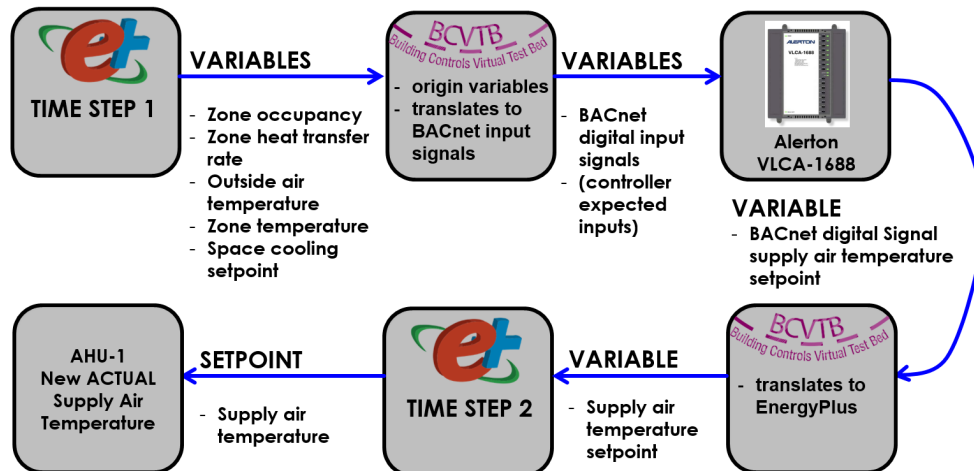


Figure 2.3: Illustration of communication of expected controller inputs indicated in Table 2.2 as required for desired output T_{SASP} (AV-19).

importance are AHU system temperatures required for supply air temperature (T_{SA}) and are shown in Figure 2.4. These temperatures include the return air temperature (T_{RA}), mixed air temperature (T_{MA}) and outside air temperature (T_{OA}). The logic required for a correct SAT signal is explained by referencing two figures, Figures 2.6 and 2.5 which are examples of the visual logic used for programming Alerton controls.

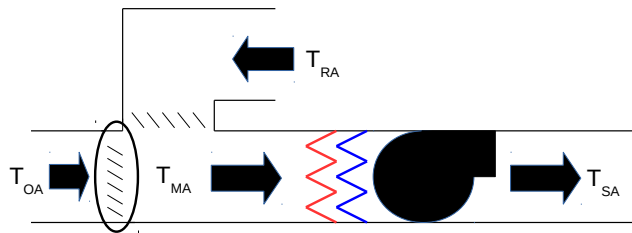


Figure 2.4: AHU key control parameters including supply air temperature (T_{SA}), return air temperature (T_{RA}), mixed air temperature (T_{MA}) and outside air temperature (T_{OA}).

A pictorial representation of AV-19 as an output is shown in Figure 2.5. The required inputs for this signal are all also included in Table 2.3. The key input signals required for SAT modulation are AV-53, AV-57 and AV-58. These are the average cooling percent (ACP) as well as the maximum and minimum allowable SAT respectively. The meaning of the average cooling percent will be later in this section. The current supply air temperature is determined by use of the two input scaler block shown in Figure 2.5. This block performs a linear conversion to the ACP signal based on the other inputs, the maximum and minimum supply air temperatures. When ACP is zero, the output of the scaler is the maximum SAT setpoint. When ACP is 100, the output is the minimum SAT setpoint. Input signals between these setpoints are converted to output according to the linear relationship. Thus this control is designed to default to the maximum allowable SAT unless there is a cooling signal.

The ACP signal is created by another portion of the control loop. A selection of this

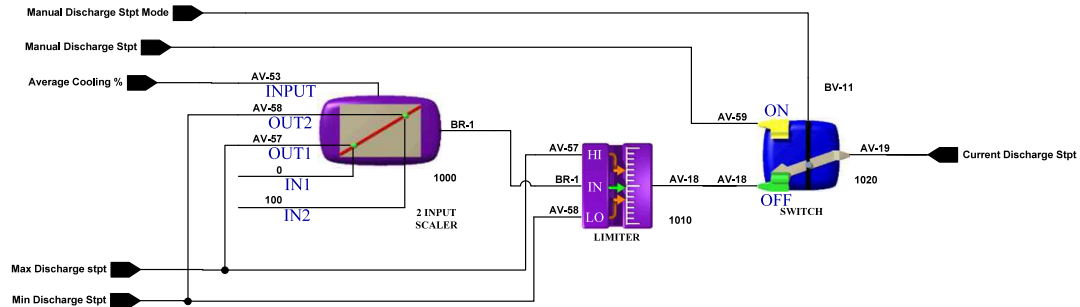


Figure 2.5: Snapshot of AHU-1 SAT control loop showing required signals for generation of a SAT SP.

portion of the loop is shown in Figure 2.6. The inputs required for the ACP are AV-51 and AV-42. The comparator block shown in this snapshot simply governs the minimum amount of cooling signal necessary for it to be passed on which in this case is anything above 0.1. An ACP output is generated when there is both a VAV cooling signal (AV-51) as well as a zone occupancy signal (AV-42). The VAV cooling signal is generated according to which zones require cooling. It is the cooling signal of each individual VAV box summed together. The VAV cooling signal is divided by the total monitored zones that are in cooling mode and this is the resulting ACP signal. There are forty five monitored zones in the actual system. The actual system monitors roughly half as many VAV boxes as there are total in the facility.

The VAV cooling signal was modeled using EnergyPlus and BCVTB in the following way. Due to the substantial amount of EnergyPlus output variables as well as BCVTB connections and configuration required to include all eighty six modeled VAV boxes, the co-simulation model was designed to simplify this task by selecting only ten sample zones to

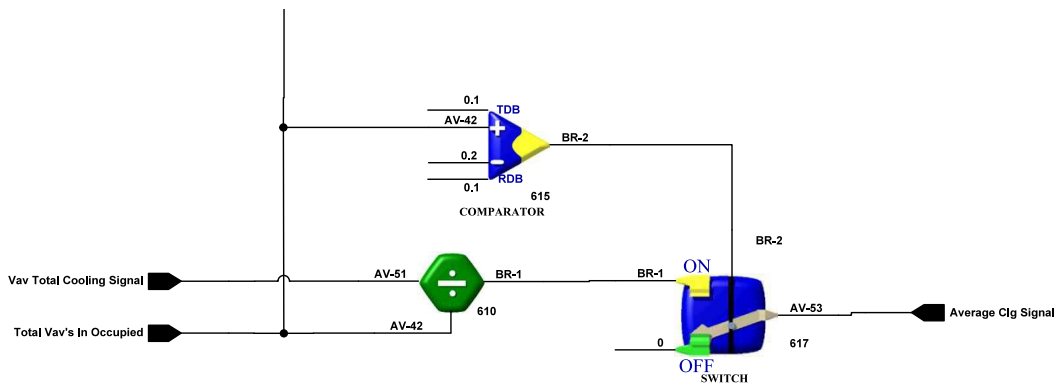


Figure 2.6: Snapshot of AHU-1 SAT control loop showing required signals for generation of the ACP signal.

derive the cumulative cooling signals from. In addition to monitoring these zones for cooling signal, occupancy monitoring was also required. Thus, occupancy as well as a particular zonal cooling signal was required as output variables from EnergyPlus.

These sample zones are chosen from various locations throughout the building in an attempt draw a sample that would produce correct control signals. The spaces selected for this purpose, their position in the building and floor area is included in Table 2.3. The choice of output variables for cooling signal as well as occupancy are 1.) Zone People Occupant Count and 2.) Zone Predicted Sensible Load to Cooling Setpoint Heat Transfer Rate. Zone People Occupant Count returns the amount of people in the zone at a particular time. Zone Predicted Sensible Load to Cooling Setpoint Heat Transfer Rate (\dot{Q}_{ZCE+}) is a metric calculated by EnergyPlus which returns the predicted amount of energy in W required to meet the current zone cooling setpoint [14]. A \dot{Q}_{ZCE+} value less than zero indicates a cooling load. Logic was added into BCVTB using comparator and Boolean multiplexor blocks to

determine when a cooling load was detected in any one of these zones. The comparator determined whether \dot{Q}_{ZCE+} was greater than zero. If this was true the Boolean multiplexor block selected a value of zero as its output. If this was false the block output was a value of one. The sum of output for each of the ten multiplexors was multiplied by ten and this result was communicated to the BACS controller as AV-51.

Table 2.3: List of sample EnergyPlus zones used to monitor occupancy and draw cooling and heating signals for use with BACS controller. Location and floor area information is indicated.

E+ Zone	Symbol	Floor	Position	Exposure	Foor Area (m^2)
101_Classroom	Z-1	Main	W end	N, S, W	274
117_118_office	Z-2	Main	SE end	S, E	30
110_seminar	Z-3	Main	E of Center	None	122
206_seminar	Z-4	Second	NE end	N	30
225B_office	Z-5	Second	S end	S, W	22
22_corridor_b	Z-6	Second	N face	N, W	148
327_classroom	Z-7	Third	E face	E, N, S	82
334_breakroom_a	Z-8	Third	E of Center	None	12
312_313_314_office_a	Z-9	Third	S and Center	S	23
301B_301C_OpenOffice	Z-10	Third	NW	N	67

The occupancy signal was determined in a similar fashion. Logic was added into BCVTB using comparator and Boolean multiplexor blocks to determine whether a signal value of one should be reported for a particular zone. If the number of people reported by the EnergyPlus output variable was greater than 0.1, the zone was considered occupied, and the multiplexor sent an output of one. All of these values were summed to calculate the amount to send as AV-42 for the total VAV's in occupied signal. The effects of these underlying control signals on the T_{SA} modulation are discussed in the following section.

2.3.6 Controller affect on co-simulation execution

Due to requirements of certain restrictor blocks in logic used in the Alerton controller, only simulations ran using one minute timesteps produced what appeared to be correct results. The effects of manipulating the restriction condition setting in these blocks were quickly studied by inspection of timing between signals in results of co-simulation. This brief analysis of these effects indicated that leaving the default setting at a value of one

corresponded to a timestep of sixty seconds on the simulation side. Co-simulations executed using one minute time steps with controller-in-the-loop were significantly longer in duration than those with fifteen minute timesteps indicated in [28]. An annual simulation took a little over a week to run to completion using a one minute timestep. Effects of synchronous changes either in BACnet logic or co-simulation setup was not a topic of detailed study for this research. Rather than synchronizing the BACnet signals by manipulating this logic, the controller logic was left intact and as result a longer simulation execution time was necessary. Thus one minute time steps were used for both simulation cases.

2.4 Results and discussion

Results from annual co-simulations from two cases, X and Y, are discussed in this section. In Case X the Alerton VLCA-1688 directly controls T_{SA} for the facility's primary AHU. In this case the modulation range for the SAT low and high limits was specified as 10.0 and 15.6° C respectively. Case Y is an EnergyPlus simulation which is not affected by an external interface and the T_{SA} is held constant at 12.8° C. Examples of the effects of underlying control signals in Case X are first discussed. Energy results from both cases are included at the end of this section where they are compared and contrasted.

2.4.1 T_{SA} modulation in Case X and underlying signals

Results for Case X show a close relationship between EnergyPlus and BCVTB processed inputs to the Alerton controller for AV-53 and AV-42 and T_{SA} . Plots of T_{SA} output signals for AHU-1 are shown in Figures 2.7 and 2.8. Figure 2.7 shows the relationship between AV-53 and T_{SA} . This relationship can be compared by contrasting the trend of T_{SA} with a plotted trend of the underlying variable used to produce AV-53, \dot{Q}_{ZCE+} . Periods of collaborating cooling loads correspond closely with modulation of T_{SA} to lower temperatures. Similarly contrasting occupancy trends with T_{SA} in Figure 2.8, occupancy also has an apparent affect

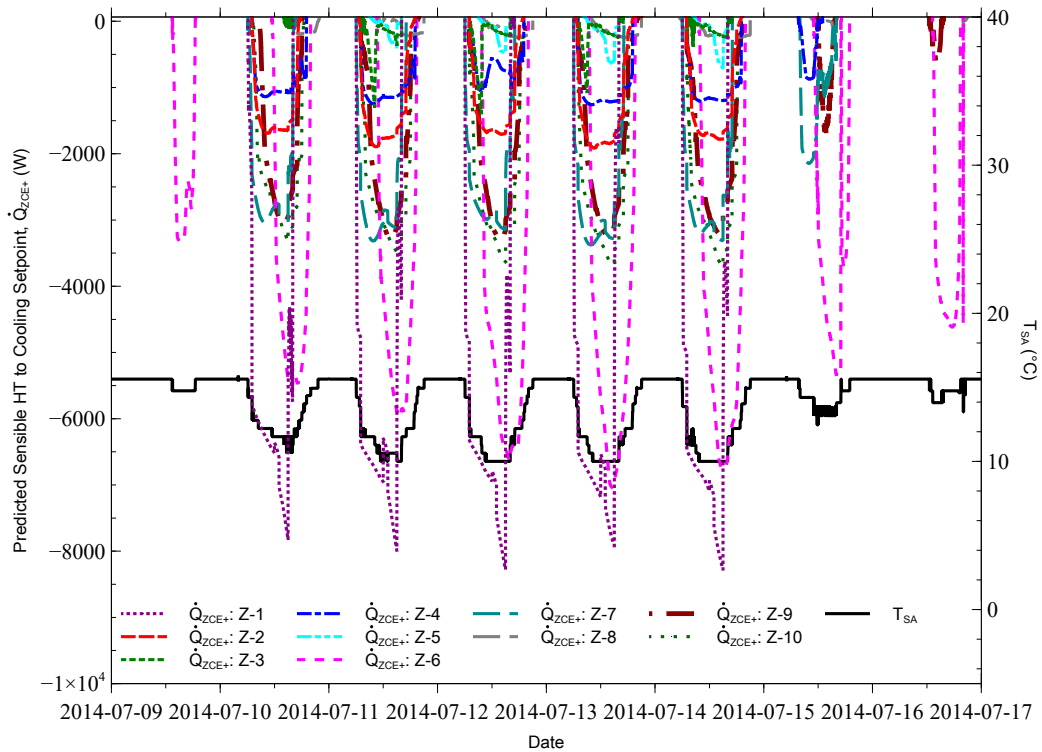


Figure 2.7: Controller in the loop modulation of AHU supply air temperature T_{SA} for Case X for a one week period in July (Jul. 9-16). Units of temperature are $^{\circ}$ C. Relationship between \dot{Q}_{ZCE+} and T_{SA} is highlighted for a summer period showing reduction in T_{SA} where cooling load occurs. \dot{Q}_{ZCE+} .

on this signal. The effect of occupancy appears as an inverse relationship. In general periods of increased occupancy correspond to the decreases in T_{SA} . While not included in either of these plots, as expected, increases in cooling load and low modulation of T_{SA} strongly correlates to increases T_{OA} for this summer period. The relationship between T_{SA} and T_{OA} for the same period is included in a later comparison in this section shown in Figure 2.10.

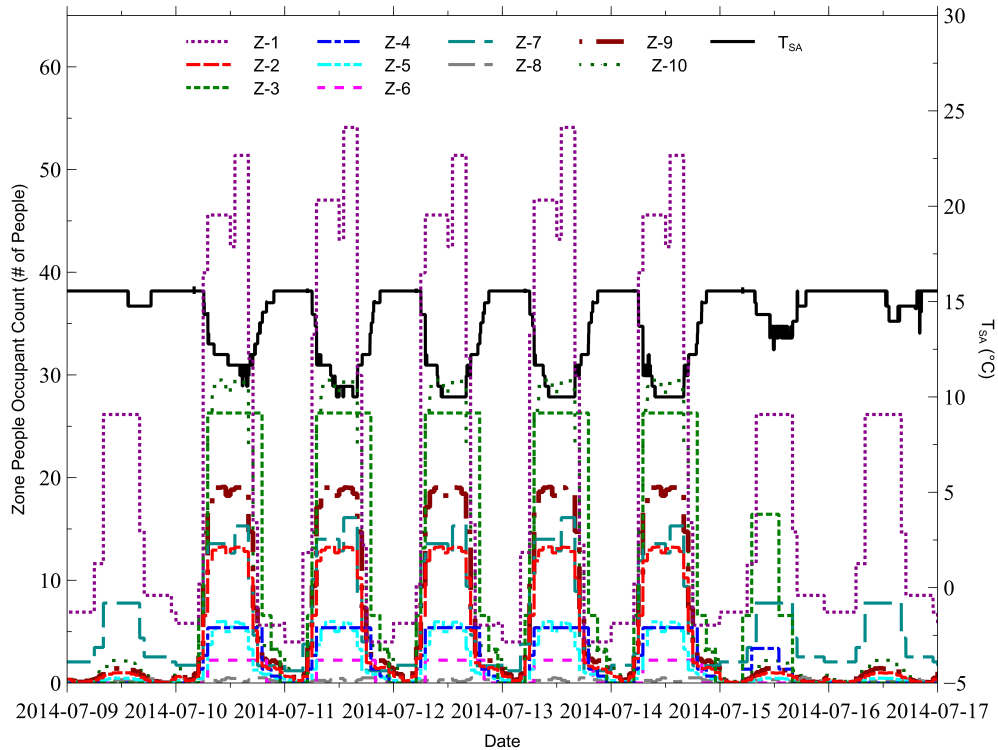


Figure 2.8: Controller in the loop modulation of AHU supply air temperature T_{SA} for Case X for a one week period in July (Jul. 9-16). Units of temperature are $^{\circ}\text{C}$. Relationship between zone occupancy and T_{SA} is highlighted for a summer period showing reduction in T_{SA} where occupancy increases.

A similar situation is examined by the results shown in Figure 2.9 but for a period within a winter month from the same simulation. Figure 2.9 shows T_{SA} response for a week in January where the relationship between this response and \dot{Q}_{ZCE+} for two of the ten sample zones is highlighted. As seen, there are certain periods where cooling loads occur in January. Modulation of T_{SA} to lower temperatures also occur during these periods.

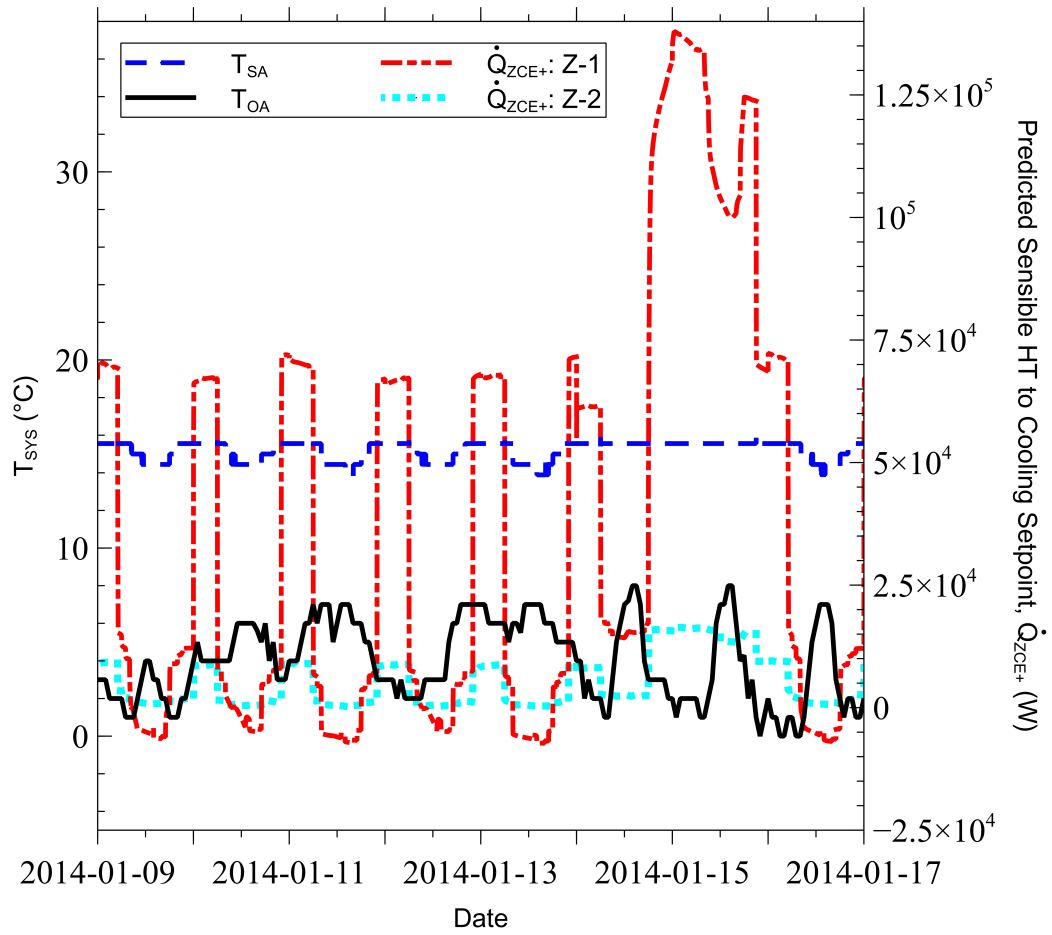


Figure 2.9: Controller in the loop modulation of AHU supply air temperature T_{SA} for Case X for a one week period in January (Jan. 9-16). Outside air temperature T_{OA} is also shown. Units of temperature are °C. Relationship between \dot{Q}_{ZCE+} and T_{SA} is highlighted for a winter period showing occasional reduction in T_{SA} where cooling load occurs. \dot{Q}_{ZCE+} signals are only included for two of the ten sample zones.

2.4.2 Comparison of T_{SA} response, Case Y versus Case X

A simple comparison of T_{SA} between cases Y and X are shown in Figure 2.10. Figure 2.10 shows a single week from the simulated year where T_{SA} is held constant in Case Y. Modulation from Case X is identical to similar plots shown earlier except T_{OA} is included on the plot to demonstrate the relationship between T_{SA} and outside temperature changes.

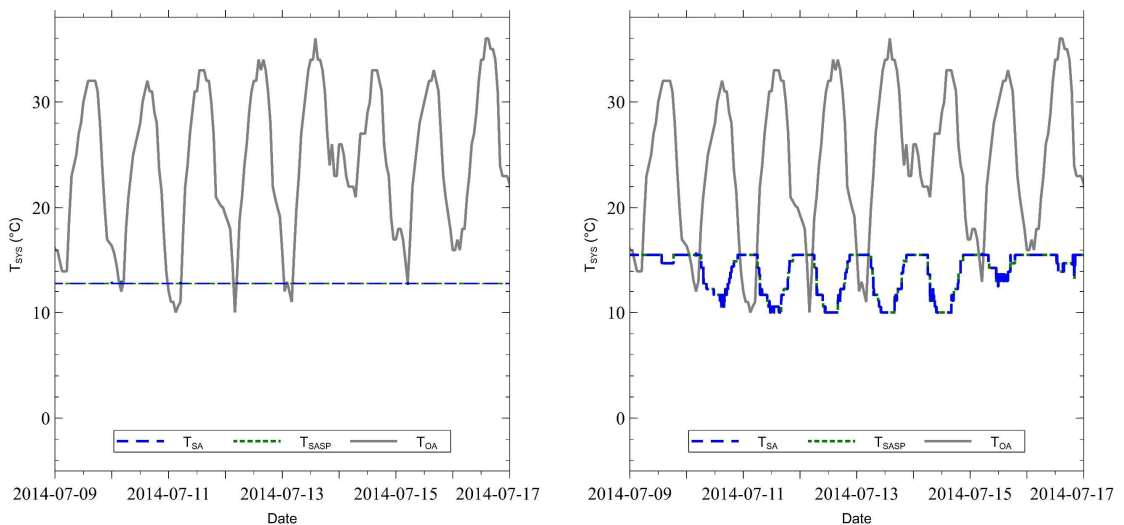


Figure 2.10: Comparison of T_{SA} response for cases Y (left) and X (right). Case Y shows constant T_{SA} response while Case X shows a modulating response.

2.4.3 Energy end use comparison

A net reduction in total annual facility energy occurs between these cases as shown in Table 2.4. The net reduction was about 9 MWh (0.6 %). Although the less than one percent reduction appears insignificant at first glance, energy tradeoffs demonstrated by this simulation are promising.

In Figure 2.11 it is apparent that the largest savings in energy between these simulations is a net reduction in 131 MWh (19%) for heating energy. Of course, this is also offset by

Table 2.4: Comparison of total facility energy simulated for cases Y and X.

Total Facility Energy MWh	
Y	X
1540	1531

a 115 MWh (42%) increase in cooling energy. There is a small reduction in fan energy of about 1 MWh (2%) as well as an increase of 8 MWh (65%) for pump energy between these cases. Values for end uses of each case are shown in Figure 2.12. Percent changes for all modeled end uses in these cases is shown in Table 2.5. The largest apparent changes based on this metric as mentioned are increases in pump and cooling energy from cases Y to X.

Based on these results and contrasting the cooling load trends between January and July

Table 2.5: Percent change in energy end uses. Reductions shown from Case Y to X, Parentheses indicate (Increases).

End Use	Percent Change
Interior Lighting	0
Interior Equipment	0
Fans	2
Pumps	(65)
District Heating	19
District Cooling	(42)

shown in Figures 2.9 and 2.7, it is likely that the benefits of a decreased heating load using T_{SA} modulation in winter months would be desirable while maintaining either a constant 12.8° C setting or lower modulation range would be advisable in summer months.

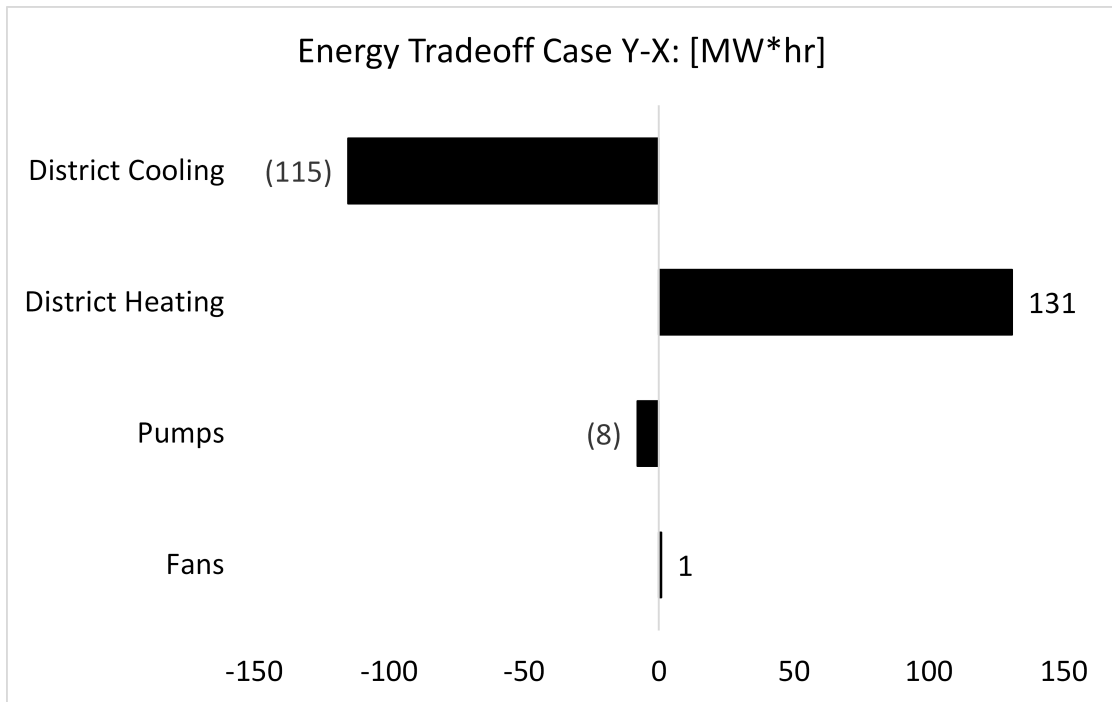


Figure 2.11: Tradeoff in selected energy end uses in MWh showing reductions from Case Y to X. Results are for an annual run period. (Tradeoffs resulting in zero percent change are omitted). Values between parentheses indicate energy increases.

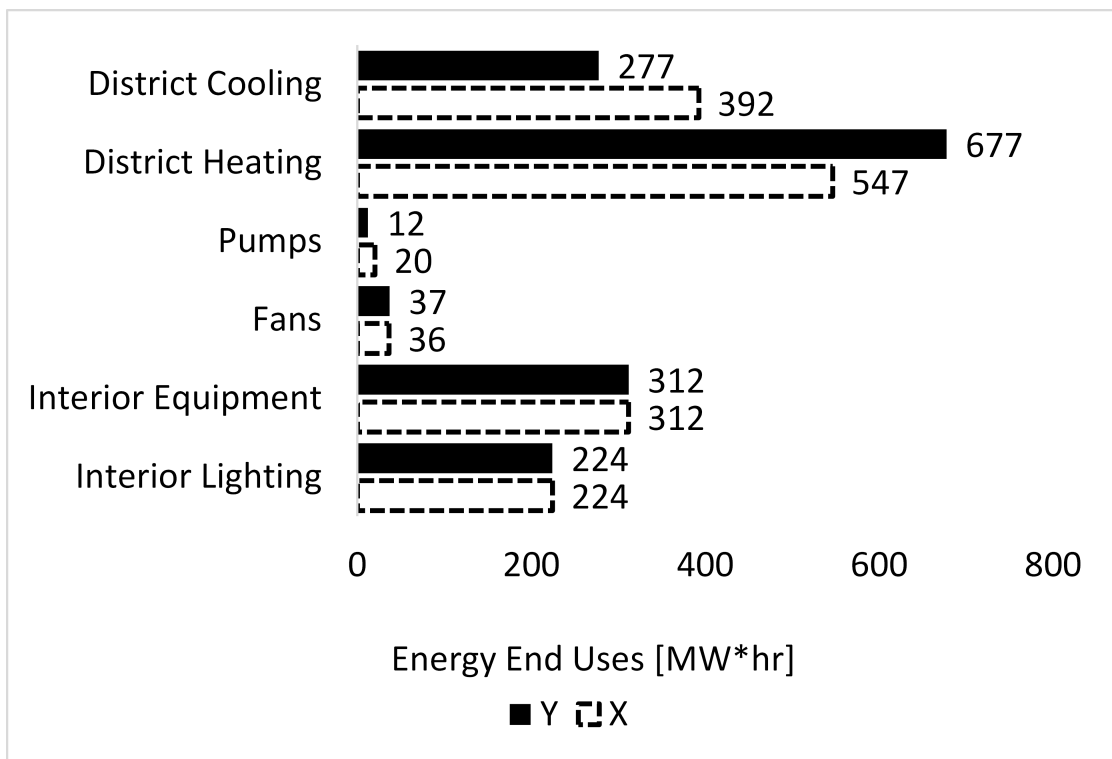


Figure 2.12: Comparison of energy end use between cases X and Y.

2.5 Conclusion

Communicating control signals from energy models to relay appropriate DDC signals to BACS controllers is not currently as simple as plug and play. In addition to the typical tasks required to setup a BCVTB control loop as discussed in [25], [24] and [16], currently additional strategies must be developed in order to communicate signals in line with controller expectations. An example strategy for communicating correct controller signals for T_{SA} using co-simulation has been demonstrated. A similar approach for communicating control signals for economizer damper position has been demonstrated in [28]. While other functions of simulated AHU operation may be controlled using similar techniques, an interesting aspect of AHU control that is not currently possible is regulation of supply or return fan speed for controlling rate of airflow. Although using the co-simulation model we developed for fan speed optimization was not possible, testing this would have been of interest for this study. Control techniques for saving energy may have been demonstrated through reset of minimum airflow in the system to an even lower level at times of unoccupancy. Another way could have been optimizing fan speed for typical operation through modulation as well as for setback situations. Through this research it was discovered that EnergyPlus does not as of this writing have a convention for control of AHU fan speed using an external interface such as BCVTB.

In results from [28] it was apparent that EnergyPlus by itself performs a more idealized simulation of economizer operation than the study test controllers. This was demonstrated by results which showed the cooling energy in the EnergyPlus only simulation was 3% less than the Alerton based co-simulation. Thus the difference in efficiency in cooling energy demonstrated estimated by the EnergyPlus results could be exaggerated by up to 3%. Even still, the modulation scheme for T_{SA} demonstrated in this study predicts up to 19% savings for heating energy. Accounting for this exaggeration of EnergyPlus idealized economizer efficiency and aforementioned results from this study, the benefits of lower modulation range

in summer months and the benefits of an increased modulation range in winter months, it is estimated that up to 124 MWh (7%) savings in total facility energy would be realized. This would be the result of increasing the modulation range for T_{SA} by up to 2.8° C when cooling loads are not anticipated for extended periods of time and allowing for an economizer cut-off temperature of 12.1° C.

CHAPTER 3

DYNAMIC PROGRAMMING AND VIRTUAL COMMISSIONING OF BUILDING CONTROL SYSTEMS THROUGH CO-SIMULATION

3.1 Abstract

Energy models are constructed and linked to a building controller network including multiple building controllers. These controllers are used to virtually control multiple air handling units in a controller-in-the-loop co-simulation using two different model representations of a facility. The challenge of programming and controlling constant volume air handling units with no zone reheat is examined using this technique. Both reduction of unmet heating set-point hours during occupied times as well as effects on energy usage are examined. Findings indicate that adjusting system performance for approaching zero unmet hours for all zones during occupied times may result in up to 30% increase in energy use.

3.2 Introduction

Programming and configuring controllers for building systems are often arduous tasks requiring significant time for participants in the highly competitive commercial controls contracting industry. Frequently issues arise where insufficient time has been spent programming and commissioning building controls resulting in energy and environmental control performance below the intent of project designs and specifications. In these situations up to 30% of energy consumption may be wasted by inefficiencies [3]. Adverse effects to the building environment may include poor indoor air quality or thermal comfort issues. Commissioning of building controls is a process employed to diminish these issues and is initially performed by installing contractors but is also an ongoing effort which involves building operators.

A building automation and control system (BACS) is the application of an intelligent net-

work of computerized controllers and other electronic devices for control of building lighting, Heating Ventilation and Air Conditioning (HVAC) and monitoring of various other systems. Buildings are greatly dependent on these controls for effective management of energy consumption. Direct digital control (DDC) is the automated control of a condition or process by a digital device. DDC solutions function under the umbrella of a particular BACS communication protocol such as the Building Automation and Control Network (BACnet) of which a large portion of all BACS products are compatible. Manufacturers of BACS's offer both configurable and fully programmable products. Configurable controllers typically only allow for user adjustment of select configuration points and setpoints. Configurable controllers require only minimal configuration for each implementation, while fully programmable controllers typically require additional configuration with preparation of customized logic that must be tested and debugged in each implementation. The additional complexity and resulting increased time required for implementations of customized logic at each project increases the likelihood for system performance below the intent of design and specifications [7].

Most BACS's in typical use are fully programmable, allowing for any number of control sequences to be programmed into the controller. This allows for implementation of advanced control sequences which when appropriately utilized will help building systems meet or exceed requirements for energy and environmental standards. Control sequences for projects are typically outlined by design engineers and controller programming is completed by DDC programmers. In [7], Hydeman, et al. outline the need for development of standardized high performance and optimized control sequences that can be pre-programmed into a configurable controller. This is suggested as an ideal means to obtain the benefits of configurable controllers without sacrificing system performance. Regardless of which controller option continues to dominate the market, effective development of vetted control sequences and pre-programming efforts may be enhanced by use of automated tools linking controllers to calibrated energy models.

There is a need for vetted methods and tools for adequately testing control sequences and

controller programming in an automated fashion. The extent to which control sequences can be adequately standardized for particular buildings, systems and climates will largely depend on how well they are evaluated against an appropriate representation of the physical reality. In [8] and [5] it is demonstrated that calibrated energy models can be powerful aids to assist in the commissioning process. In [28], proof-of-concept of pre-commissioning controllers is demonstrated by linking a BACnet compatible controller to a calibrated energy model which approximates the building envelope and HVAC system of a 4,600 m^2 three-story building. The energy model was developed using the EnergyPlus software and the communication link was established between the model's primary air-handling unit (AHU) and the physical controller by means of the Building Controls Virtual Testbed (BCVTB) [16]. The communication was established such that the signal for economizer damper position was provided to the EnergyPlus simulation by the BACnet controller in lieu of the program's default controller. In this fashion, commissioning the BACnet device for economizer operation was carried out completely virtually. Through virtual commissioning efforts, it was discovered that a combination of adjustments in configuration settings would result in 12% (190,000 kWh) of energy savings per year.

In the present study the possibility of using both BCVTB and calibrated energy models to assist with programming, configuration and testing programming for BACSs was investigated. Also examined was the feasibility of expanding the scale of implementation of virtual commissioning to include control of multiple units as well as including multiple controllers in the loop in a co-simulation. Multiple co-simulation situations are discussed for run periods of both full months as well as shorter three day periods. DDC programming used in co-simulations for this study differed from the programming used in the actual control network for the physical HVAC system used by the facility. One key difference includes direct communication of a desired supply air temperature (SAT) as a control signal for each AHU. Another difference is control of multiple AHUs from a particular controller. The actual logic used for control of the physical systems was designed to modulate SAT indirectly through

control of heating or cooling coil valve positions. EnergyPlus does not currently support control of AHU coil valve position using an external interface such as BCVTB, whereas desired SAT may be controlled in this fashion. Changes to controller logic were also required to handle control of multiple AHUs from a particular controller. Further changes to controller programming and configurable parameters are made and tested using controller-in-the-loop co-simulation. Developing custom AHU logic for this project allowed for study of the usefulness of co-simulation as a tool to test controller programming and control sequences. Findings based on these and other smaller changes are discussed in detail throughout the duration of this paper. Control challenges related to the particular HVAC system employed in simulation and actuality are also discussed. The HVAC system used by the actual facility and the energy model consists of multiple constant-air-volume air handling systems with no reheat air terminals at zones. The absence of reheat capability at the zonal level presents some difficulty in adequately controlling room temperature of spaces linked to a unit.

In particular two separate sets of cases are discussed for full month co-simulations run for January and August respectively. Through an iterative process changes to controller programming were made in order to meet setpoints and produce correct control of simulated systems. Co-simulation was performed to analyze effects caused by various changes. Results from testing performed to understand the behavior of the energy model aside from a co-simulation environment are first discussed in some detail in order to provide a reference frame for differences between two separate models that were used independently for January and August cases. This preliminary testing also helped gauge the adequacy of the energy model at effectively regulating zone air temperatures outside of the co-simulation environment.

3.3 Case study background

The building selected for this study was the Hartung Theatre on the University of Idaho campus in Moscow, Idaho. The building has a net conditioned area of 2,000 m^2 and is three total levels consisting of an auditorium spanning two levels with a basement below. The

auditorium is surrounded by a lobby and various other spaces including theatre preparation, activity, and facility management rooms. Figure 3.1 provides a snapshot of the actual facility geometry compared to the modeled geometry.



Figure 3.1: Comparison of actual (left) to modeled geometry (right). Picture of actual geometry is courtesy of Google Satellite Imagery.

3.3.1 HVAC system

The conditioned area is served by a total of five constant-air-volume (CAV) AHU's with dry bulb economizing, each serving multiple zones by means of no reheat air terminals. Each unit is equipped with hot and chilled water coils providing air conditioning to various facility zones. Each unit supplies a constant rate of supply air, but the operational rate of supply air varies from unit to unit. A comparison of actual, design and modeled supply airflow is included in Table 3.1.

Table 3.1: Comparison of AHU supply fan airflow contrasting actual air balance data with facility design and modeled values for five AHUs.

Unit	AHU Supply Airflow $\left(\frac{m^3}{s}\right)$			
	Actual	Design	Model Q	Model R
AHU-1	7.2	6.8	6.8	6.3
AHU-2	2.4	2.4	2.1	1.9
AHU-3	2.8	2.8	2.3	2.2
AHU-4	1.5	1.3	1.4	1.3
AHU-5	2.0	2.0	2.0	1.4
Total	15.9	15.3	14.6	13.1

The reason for the difference in AHU supply airflow rates between models Q and R is the option for autosizing airflow rates was selected in the OpenStudio application in Model

R. AHU-1 includes both a supply and return fan (RF), while AHU-2 through AHU-5 use only supply fans. Exhaust air is handled by eight centrifugal exhaust fans (EF's) serving various zones as well as AHU-1. A natural gas boiler and an electric chiller supply the hot and chilled water to the coils of each unit. The reasoning behind the use of the two energy models noted in Table 3.1 as well as differences between them are discussed in a later section.

3.3.2 Controllers

In addition to the AHU's controlled by the BACS various other HVAC equipment are also controlled including a return fan (RF-1), boiler, chiller, domestic hot water pump (DHWP), and seven EF units.

Table 3.2: List of items controlled in facility BACs network along with the respective device information.

Equipment	Device Model	Comm. Protocol	Make
AHU-1, RF-1, EF-1	VLC-1188	MSTP	Alerton
AHU-2	VLC-853	MSTP	Alerton
AHU-3, EF-6	VLC-853	MSTP	Alerton
AHU-4, EF-3, EF-4, EF-7	VLC-1188	MSTP	Alerton
AHU-5, DHWP	VLC-1188	MSTP	Alerton
Boiler	VLC-853	MSTP	Alerton
Chiller	VLC-853	MSTP	Alerton
EF-2, EF-5	VLC-444	MSTP	Alerton

A list of all items controlled in the network along with their respective model numbers, communication protocol, and manufacturer are included in Table 3.2. The list of physical controllers actually used in the co-simulation are shown in Table 3.3. The co-simulation employed controllers from the same manufacturer, but the specific models and quantities used are different.

Table 3.3: List of Alerton BACnet controllers used in co-simulations with respective AHUs.

Device Model	Equipment	Comm. Protocol	Make
VLCA-1688	AHU-1, AHU-2	BACnet IP & MSTP	Alerton
VLC-1188	AHU-3, AHU-4	MSTP	Alerton
VLC-1600	AHU-5	MSTP	Alerton

Actual controllers used in the building all employ master slave token passing (MSTP)

protocol and each air handling unit is handled by a separate controller. In comparison, the model used a network of only three controllers programmed with separate logic to control all five AHU's. Both the VLCA-1688 and the VLC-1188 included in the model were programmed to each control two AHU's using separated logic. This was accomplished by two independent AHU control loops on each shared controller with a particular loop serving only one AHU in the simulation. The VLC-1600 was used for the control loop of only AHU-5.

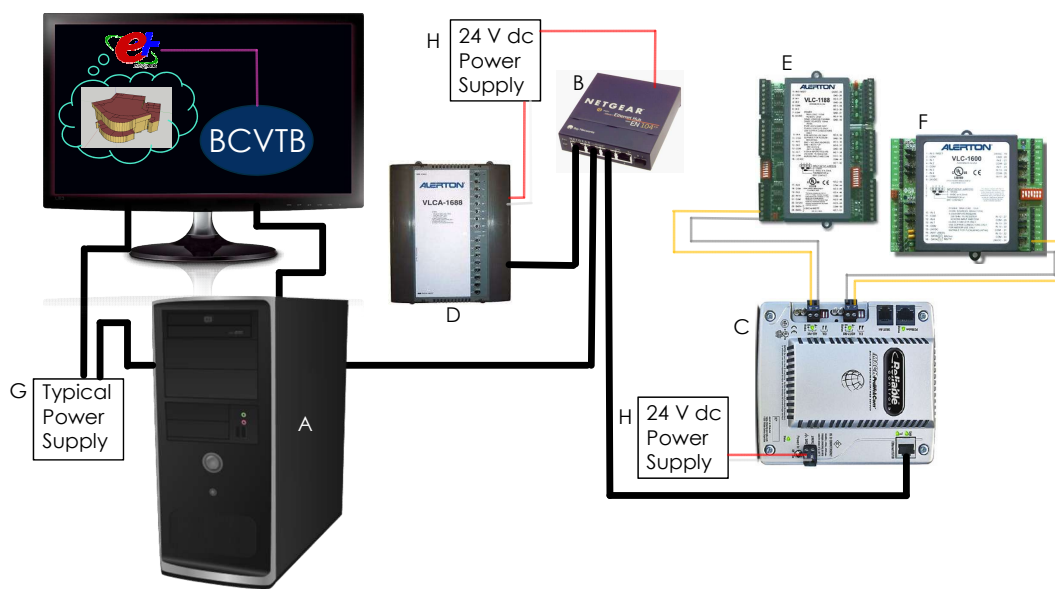


Figure 3.2: Diagram of BACnet controller network used in co-simulations showing: A.) Typical 12 GB desktop PC, B.) Netgear Ethernet hub, C.) Mach-ProWebCom MSTP to BACnet IP gateway device, D.) Alerton VLCA-1688, E.) Alerton VLC-1188, F.) Alerton VLC-1600, G.) Typical Power Supply and H.) Typical 24 V dc power supply

An illustration of the complete network setup used in simulation is shown in Figure 3.2. As shown in Table 3.3, the Alerton VLCA-1688 can communicate using both BACnet IP (via CAT-5 cable) and MSTP (via typical 18 AWG twisted shielded pair wiring). In this study only its BACnet IP capability was used. To establish communication with BCVTB all MSTP controllers used in the model were eventually converted to BACnet IP using a MSTP to BACnet IP gateway device called the MACH-ProWebCom manufactured by Reliable

Controls. The BACnet network was relayed to a typical PC with 12 gigabytes of RAM running all of the software using a typical Ethernet Hub manufactured by Netgear.

3.4 Materials and methods

Aside from obtaining the relevant equipment necessary to perform this research, completion of three critical activities were necessary to perform the co-simulation. These included 1.) constructing the energy model, 2.) creating the BCVTB model, and 3.) programming the BACnet controllers. This section provides information on the process of creating the required models and controller programming. The approach used to apply co-simulation to the problem of testing and improving DDC programming is discussed in detail. Some commentary on the level of effort required to perform certain tasks as well as the suitability of the software tools involved in co-simulation is included in order to convey the suitability of these tools to handle the problem of testing and commissioning controls.

3.4.1 Energy model

The energy model was mostly constructed in OpenStudio which is the front-end application intended for use with EnergyPlus and Radiance [14]. Use of OpenStudio to construct an energy model greatly simplifies the process. Even still developing, testing and calibrating an energy model can require a great deal of effort. The user must acquire enough accurate information about the building to produce an adequately representative model in terms of geometry, materials and equipment. Additionally, utility data is important in order to determine how well the model performs in contrast to reality. Weather data used in all modeling including co-simulations was data from an actual meteorological year (AMY) for 2014 from the Pullman-Moscow Regional Airport. An estimated 50 hours of effort went into producing a functional energy model vetted against actual utility data.

The model geometry approximates the envelope and floor plan of the actual building. A

comparison of modeled to actual geometry is included in Figure 3.1. All five CAV AHU's were modeled and appropriate zones were linked to the unit serving them in reality. The model was developed in an iterative fashion and two ultimately slightly different versions of the energy model were utilized each for a series of co-simulations using BCVTB. For Model Q, which was used mostly for simulating system operation for the full month of August, exhaust fans were also applied to the appropriate zones. Model Q included two natural gas boilers. AHU-1, AHU-2 and AHU-4 were attached to one natural gas boiler, while AHU-3 and AHU-5 were connected to the other.

Model R differed from Model Q in that the larger hot water heating plant loop supplying AHU-1, AHU-2 and AHU-4 was selected as district heating instead of a typical natural gas boiler. It also neglected exhaust fans. The reason for this difference was insufficient capacity available from the modeled natural gas boiler loop serving these units to supply the required heating energy demanded by actual controller signals. This prevented the AHUs in the loop from matching actual SAT to the signal received from the controllers throughout January simulations. Attempts were endeavored to determine why there was a lack of capacity in the boiler loop. Iterative changes to plant settings were implemented and simulations performed as tests to determine the cause. These efforts were intended to determine whether the model was simply flawed or whether other factors could be the cause. Testing seemed to indicate a solution convergence issue for this loop throughout problematic times including periods spanning multiple hours throughout the coldest weeks. Nonetheless model behavior seemed appropriate otherwise. Whether the issue is a flaw in the model or a possible bug in the software, applying the simplification of a district heating loop in lieu of the boiler loop remedied this problem. Additionally, Model R behavior is similar to results obtained using Model Q for non-problematic periods. The only difference in this respect appears to be improved functionality during periods that were otherwise problematic for Model Q. Furthermore, use of a model simplification was appropriate because energy analysis within this study is primarily concerned with effects of changing controller

programming on a baseline energy model primarily for the purpose of determining effects on individual air handling units. EnergyPlus documentation indicates that use of the district heating or cooling convention is appropriate when the plant in question is not of primary importance to the research [14]. This is the case with this research as controller effects on specific air handling units are the primary focus. This two model approach for this research would have been abandoned in favor of performing all testing with Model R, however, cases for the month of August were all run using Model Q. Due to the significant time involved performing the previous research and considering no problems were observed for meeting cooling loads with either model, research for SAT control in heating mode proceeded with Model R. Thus, this explanation for use of two separate models was necessary to provide a background for presenting results of this research.

Simulations with both Model Q and R indicated good to reasonable agreement respectively compared to actual electrical energy usage. Effects of the changes made between models Q and R are apparent in following comparisons throughout the remainder of this section. Other details of importance related to this topic as it relates to co-simulations are covered in later sections.

The following examples include contrasting of cases, Q-1, Q-2, R-1, and R-2. “Q” cases use Model Q, while “R” cases use Model R. The changes between numbered cases are simply a change to the setpoint managers of both heating plants in each model. These changes are consistent between models Q and R and are explained in this section. A comparison of monthly modeled to actual electrical energy use for both models Q and R for 2014 are shown in Figure 3.3. These are results from cases Q-1 and R-1 which use the same gamut of plant settings applied in subsequent co-simulations. Settings for heating plant setpoint schedules are discussed later in this section. The key difference between these initial cases is use of a different model. Differences between models Q and R include more reliance on autosizing features of Model R instead of so much hard sizing of air flow rates for mechanical equipment as is the case with Model Q. Additional changes include the change to district

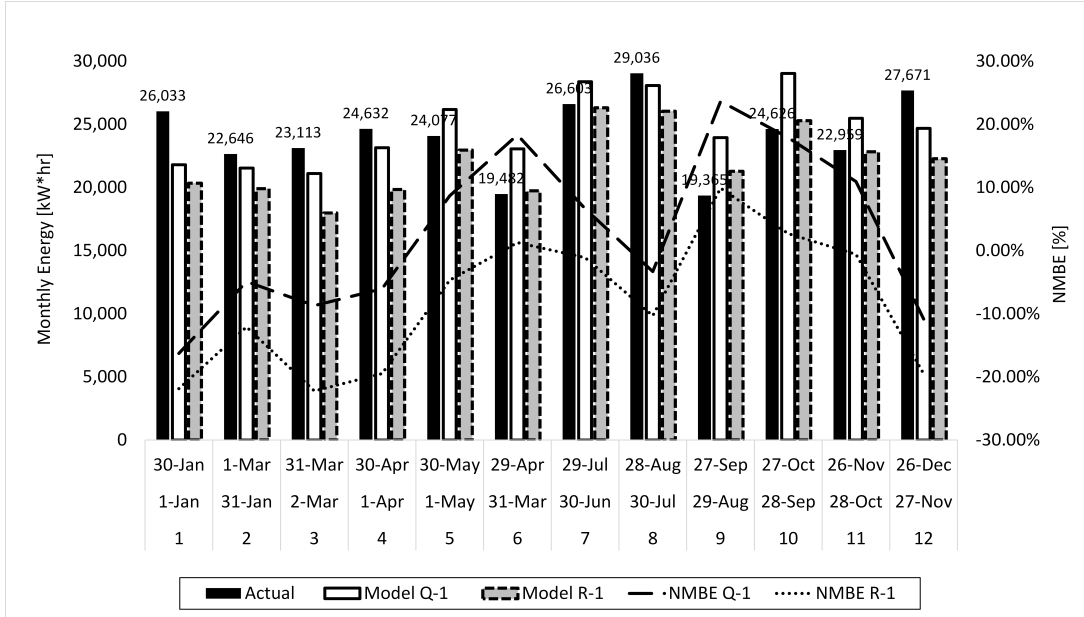


Figure 3.3: Comparison of monthly actual to modeled electrical energy use for cases Q-1 and R-1 throughout 2014.

heating for one plant as well as the fact that Model R neglects powered exhaust fans. The results indicate close agreement for electrical consumption between these cases. As seen the increases and decreases in modeled energy use between most months corresponds to the same trend in actual use. This agreement is quantified using the ASHRAE 14-2002 calibration method. ASHRAE energy model calibration requires calculations for normalized mean biased error (NMBE) and coefficient of variation for root mean square error CV(RMSE). NMBE determines whether the model comprehensively over or under predicts energy usage, whereas CV(RSME) assesses how closely monthly predictions correlate to monthly utility data. Calculations using this method indicate the values of 12.61 and -2.29 for CV(RMSE) and NMBE respectively for case Q-1. The same calculations for R-1 yield values of 14.38 and 9.59 CV(RMSE) and NMBE respectively. The guideline specifies that CV(RMSE) below 15% as well as NMBE of 5% or less indicates satisfactory correlation. Model Q attempted to model all HVAC equipment in the facility. Contrasting R-1 results with those from Q-1, monthly electrical energy is less for most months. Comparison of end uses from both cases showed a significant decrease in both cooling and fan energy from Model Q to Model

R. Cooling energy decreased by 13,567 kWh, a 22% decrease, and fan energy decreased by 18,975 kWh which was a 23% decrease. The overall decrease in electrical energy by neglecting exhaust fans and other effects by design differences does take Model R somewhat below the ASHRAE standards for calibration. A modest constant energy scaling factor would bring Model R back up to the calibration standard. There was also a 111 MWh (13%) reduction

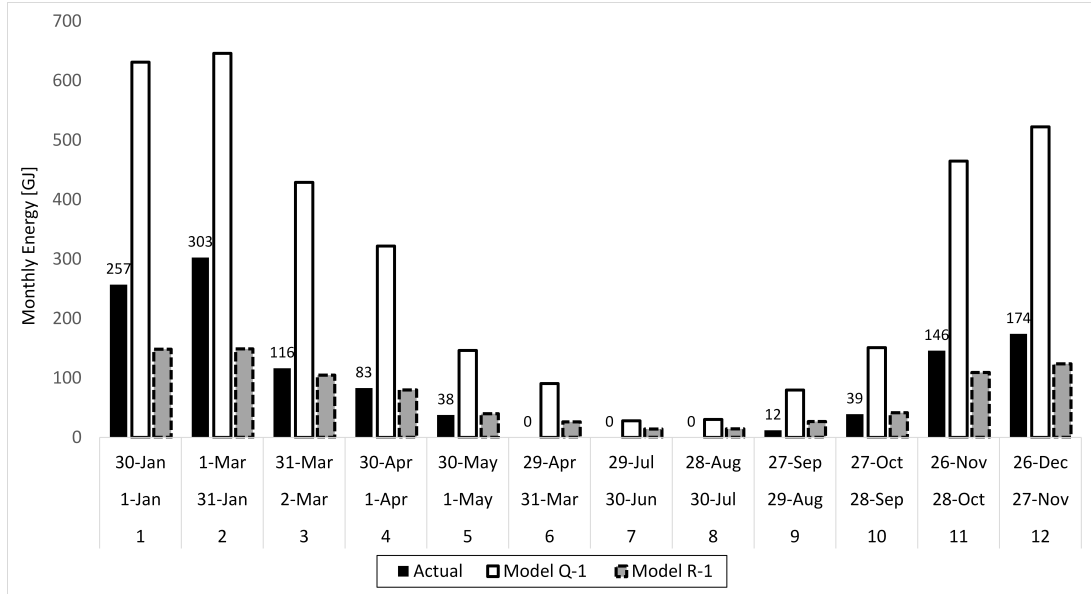


Figure 3.4: Comparison of monthly actual to modeled natural gas energy use for cases Q-1 and R-1 throughout 2014.

in heating energy between these two models. One item leading to this reduction could be the elimination of exhaust fans from the simulation in Model R. Additional differences in modeled efficiencies of district heating plant in Model R above the natural gas boiler plant loop it replaced from Model Q is another factor involved. The district heating model functions by calculating the output capacity necessary from the inlet temperature to the setpoint temperature for a particular loop using its mass flow rate [13]. On the other hand, a set of curves, efficiencies and parameters must be input by a user to model a particular boiler loop. Thus district heating is a more idealized convention and is intended for use when consequences of heating plant loops are of little or no concern [14]. Thorough investigation led to the conclusion that the district heating option was best for January co-simulations as

the model was not limited by the settings selected for a particular boiler. Results from a portion of this investigation are included in model comparisons within this section as well as later in this paper in order to provide adequate information regarding each model used in subsequent co-simulations.

Natural gas usage for heating varied substantially from the actual utility data in both cases. Model Q showed substantially higher use, while Model R showed lower usage. Recall that Model R uses district heating to supply the heating requirement for the facility's largest AHUs, thus substantially less energy due to burning natural gas is realized as expected. Comparison of these results are shown in Figure 3.4. Some reasons for the discrepancy in heating energy between modeled and actual cases are 1.) the modeling approach for availability of heating energy in the plant loop, 2.) the approach for modeling SAT in the stand-alone energy models and 3.) differences between periods of modeled and actual conditioning of the facility. Explanations for the ways in which these suggested reasons affected simulation results are supported by a comparison of two test simulations using both energy models.

Approach for modeling availability of heating energy in the plant loop

Cases Q-1 to Q-2 and R-1 to R-2 each made the same change to a setting for a setpoint manager for both heating plant loops. A setpoint manager is an EnergyPlus convention for controlling setpoints for various HVAC equipment. The setpoint manager selected for these plants shifts linearly between two desired heating temperature setpoints based on outdoor air temperature (OAT) reset. The purpose of this setpoint manager is to diminish plant based heating energy at times when heat is not required by the HVAC system. These include high and low heating plant SAT settings with linear modulation between them based on two OAT trigger points. Linear modulation is within the deadband range between the two trigger temperatures. A constant value of the high SAT setpoint is used above the high OAT

trigger point and a constant low setting of the low SAT setpoint is selected below the low OAT trigger.

Table 3.4: Settings for OAT reset setpoint manager for selected cases. Temperatures listed are in °C.

Case	SP Low OAT	at Low	OAT Low	SP High OAT	at High	OAT High
Q-1	99.4		14.4	23.9		23.9
R-1	99.4		14.4	23.9		23.9
Q-2	99.4		0.0	23.9		8.9
R-2	99.4		0.0	23.9		8.9

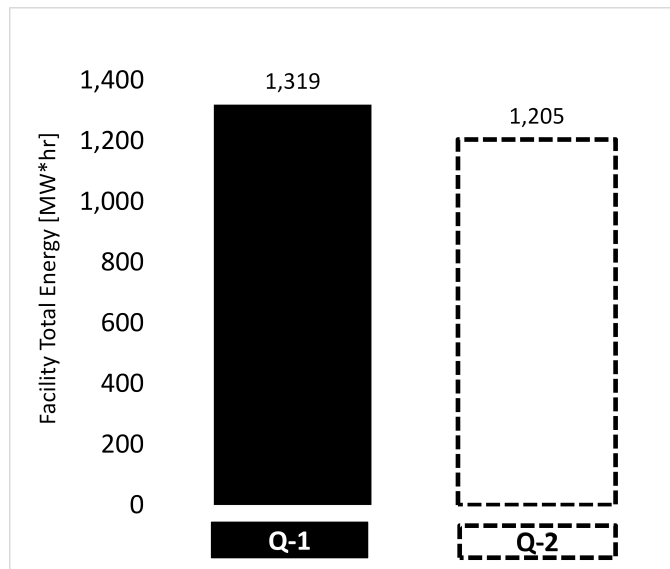


Figure 3.5: Comparison of total facility energy use simulated using cases Q-1 and Q-2 throughout all of 2014.

Cases Q-1 and R-1 both used the values shown in Table 3.4. These values affect plant temperature in the following manner. The plant loop will supply 23.9° C water when the OAT rises to or above 23.9° C. Linear modulation up to 99.4° C occurs as OAT falls to 14.4° C. For OAT below 14.4° C the plant attempts to supply 99.4° C water to inlets of unit coils. These are the settings used by the numbered “B” cases for January co-simulations using Model R which are explained later. Cases Q-2 and R-2 use values also included in Table 3.4. The change between these cases is a reduction in both the low and high OAT

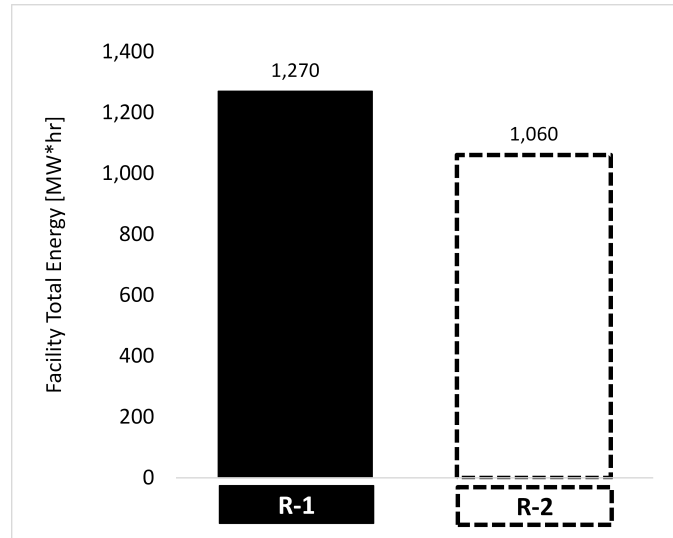


Figure 3.6: Comparison of total facility energy use simulated using cases R-1 and R-2 throughout all of 2014.

triggers. Running simulations for both models across cases 1 and 2 yielded the following results.

Figure 3.5 shows a comparison of annual energy required by the facility in simulation cases Q-1 and Q-2. A reduction of 115 MWh (8.7%) is realized by the adjustment in settings. Contrasting Figure 3.5 with Figure 3.6 which shows results using Model R for identical parameter changes, we see a 209 MWh (16.5%) reduction between these cases. The additional energy reduction across cases using the model with the district heating loop is indicative of the differences in the modeling approach. Figures 3.7 and 3.8 further contrast these differences in energy use by focusing on individual end uses. As seen in these figures each model realizes a slight reduction in cooling energy in addition to the reduction in heating energy. The reduction for cooling in Model R between cases is likely enhanced by the effects of modeling district heating. Besides the reduction in heating energy between cases, most other uses remain almost constant. Regardless of model or case, the actual facility boiler likely does not experience near the demand that is required of modeled plant loops, especially in simulation of winter months. This facility functions as a university theatre and performing arts center that is not utilized for certain periods throughout winter months.

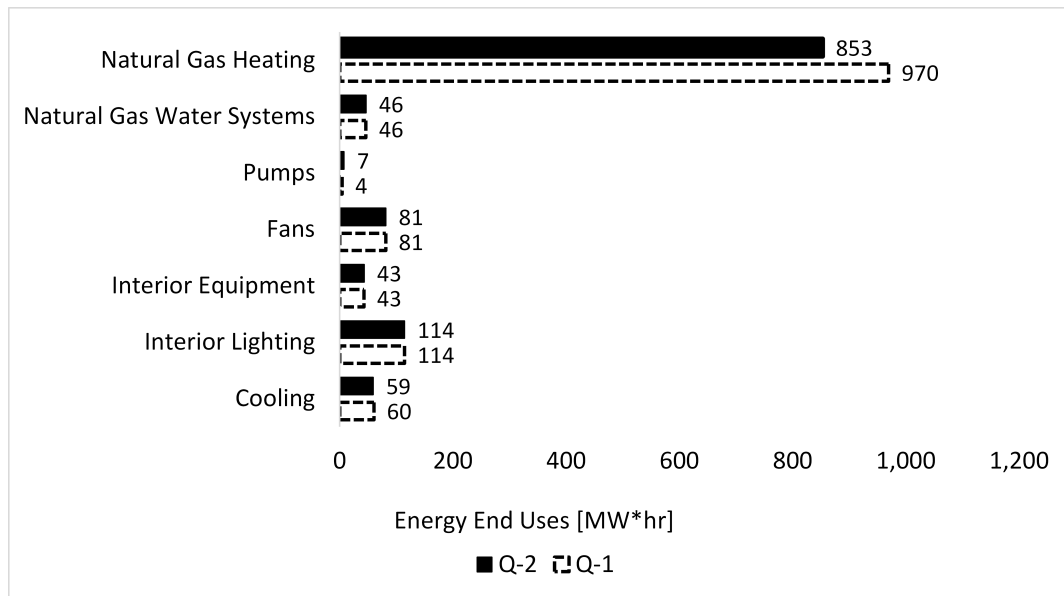


Figure 3.7: Comparisons of energy end uses simulated using cases Q-1 and Q-2 throughout all of 2014.

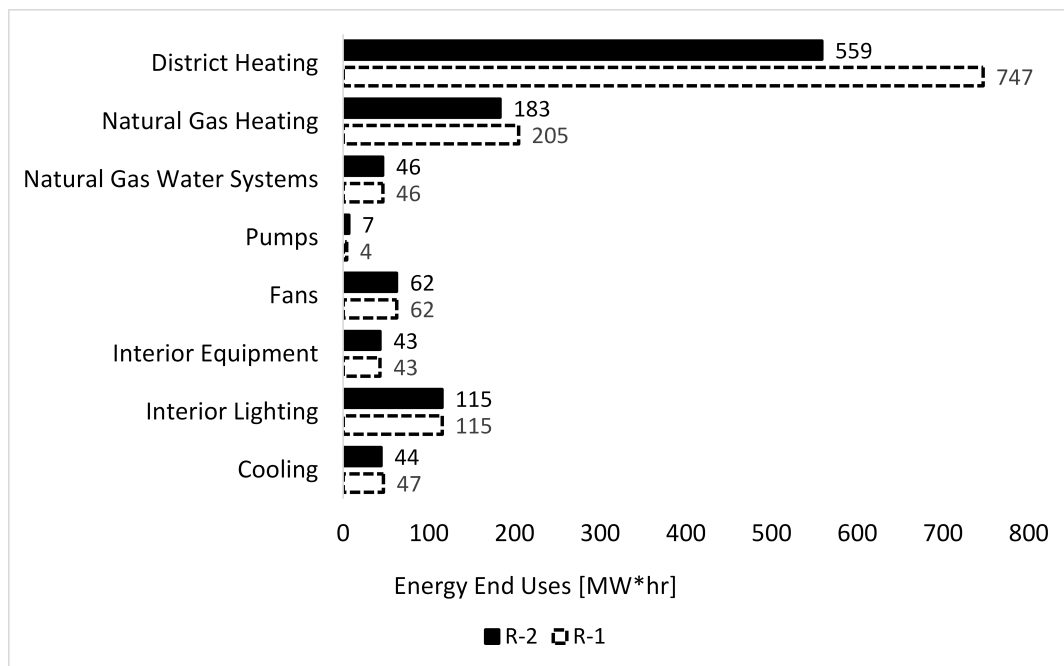


Figure 3.8: Comparisons of energy end uses simulated using cases R-1 and R-2 throughout all of 2014.

Results from these cases provide an example where a change to management of heating plant supply temperature to AHU coils had a significant effect on simulated energy use. It is possible that adjusting plant settings and modeling periods of operation more closely match actual operation would improve consistency the model and reality. However, further extensive investigation into the exact relationships between modeled and actual plant settings and behavior is beyond the scope of this research. The purpose of these comparisons is to provide some level of understanding of the behavior of the model due to differences in design. They also provide some insight into the suitability of the respective models for examining iterative changes to controller programming using co-simulation. Effects related to these changes made between the two models appear to show some consistency. For instance, reducing the OAT low and high triggers for the setpoint manager result in a comparably similar change in in cooling energy between cases Q-1 and R-1 as that which occurs between Q-2 and R-2. From Q-1 to R-1 there was a reduction of 13,567 kWh (23%) and from Q-2 to R-2 there was a 14,911 kWh (25%). Some discrepancy in percent changes may be accounted for by effects noted previously due to replacing a natural gas boiler loop with district heating.

Differences between periods of actual and modeled conditioning of the facility

The model takes a simplified approach to schedule of HVAC heating and cooling use. Ultimately, it was determined that models used in co-simulation would operate according to a typical working week throughout simulation periods. Thus, there are periods of nighttime and weekend setbacks for setpoints, but setpoints for all conditioned spaces are geared for comfort for occupied times throughout every week. The intent of this approach was to make effects of changes in controller programming more apparent in results. Zone heating setpoints were intentionally simplified in the model to take a blanket type approach for months requiring heating. While setbacks for periods of daily unoccupancy are used, entire periods of unoccupancy greater than one day typical to a university setting are not modeled.

The actual facility has periods where some or all zones are not heated much above 16° C. Whereas one goal of co-simulations for January was to keep all zones up to a minimum specified setpoint.

Approach for modeling supply air temperature in the energy model

In lieu of co-simulation the energy model is subject to EnergyPlus conventions for regulating AHU supply temperatures. The option selected for SAT regulation in the EnergyPlus stand-alone simulations was an option based on OAT reset similar to that chosen for use with the heating plants. This method is near synonymous with a guess and check method for the correct SAT to regulate space temperature for several independent zones. Modeling other HVAC systems, such as variable air volume (VAV) scenarios, a user can employ zonal reheat of air at air terminals which helps to regulate zone air temperature appropriately in simulations. There are no conventions particularly well suited for effective regulation of SAT for CAV systems with no reheat air terminals in EnergyPlus. The setpoint manager which modulates SAT based on OAT reset seemed to be the most flexible option available. Selection of a building with CAV AHUs supplying conditioned air with no reheat air terminals provided an opportunity to demonstrate the usefulness of co-simulation as an appendage to typical energy modeling as well as demonstrating its ability to troubleshoot control issues typical to these systems. Whatever heat energy remains in air when it reaches a particular air terminal is what is supplied to the zone in resides in. Thus from a comfort standpoint, the SAT as discharged from the AHU would ideally be optimized to supply comfortable temperature conditions to a maximum amount of zones linked to it. This is a real control problem that is not easily solvable even in the real world. This problem is also not handled well with default options available in EnergyPlus at least without a substantial amount of effort in contrast with the quality of results. This observation was made through substantial preliminary testing. Results from case R-1, for instance, which uses more heating energy than case R-2, shows twenty five zones with periods of unmet heating setpoint and twelve of

these instances are for over 500 hrs. While using Model R, which adequate heating capacity in its largest heating plant loop, in conjunction with an AHU setpoint manager with an OAT low trigger set sufficiently high enough to cause a ample elevation of space temperatures quickly enough to eliminate periods of unmet heating setpoint, this approach also tends to cause the reverse problem of overheating above desired cooling setpoints. These controls are simply too rudimentary to efficiently determine a reasonable solution representative of actual system regulation of SAT. As the control of AHU SAT within EnergyPlus outside of a controller-in-the-loop environment was not a primary focus of this research, use of co-simulation was instead employed to determine more reasonable control solutions.

Suitability of the model for subsequent co-simulations

Electrical energy in model simulations trend reasonably well compared to use indicated by actual utility data. Even with moderate changes to the model as in the differences between models Q and R, this trend seems to remain. Discrepancies in modeled to actual heating energy as well as differences in the behavior of Model Q and Model R have been discussed in some detail. Differences between modeled and actual energy use can reasonably be explained by 1.) the modeling approach for availability of heating energy in the plant loop, 2.) the approach for modeling SAT in the stand-alone energy models and 3.) differences between periods of modeled and actual conditioning of the facility. The implementation of Model R for subsequent January co-simulations was necessary to ensure meaningful comparisons could be made for results based on changes to programming (e.g. Figures 3.15 and 3.16 from the results section).

3.4.2 BCVTB model

BCVTB was the key to co-simulation. It facilitates the communication between all other software and hardware in the loop. Because of this, initialization of all co-simulations occurred within the BCVTB platform. Surface level analysis was also performed within the

application. Prior to running co-simulations with an energy model substantial development within the BCVTB platform is required. EnergyPlus input data files (.idf) were exported from OpenStudio and changes necessary to prepare the files for use with BCVTB were made using a notepad application.

Communication

The process for establishing full loop communication from BACnet Controllers to BCVTB and BCVTB to EnergyPlus are described in detail in [25], [24] and [16]. As of this writing, the current state of the BCVTB software requires the user to perform significant manual linking of signals within its graphical interface in order to establish full loop communication and simulate control all equipment involved. Also, a significant level of manual manipulation of EnergyPlus .idf files is required in order to complete the process. Additional use of extensible mark up language (.xml) files is required in order to include hardware like BACnet controllers in the loop.

The BCVTB model itself was designed to gather the required controller inputs supplied from both EnergyPlus and within BCVTB necessary to produce BACnet controller outputs. The BACnet outputs required from the controller were specific EnergyPlus expected signals including supply air temperature setpoint and economizer damper position. System inputs included variables supplied from EnergyPlus such as temperatures including outside air (OSA) temperature, supply air temperature (SAT), mixed air temperature (MAT) and return air temperature (RAT) as well as zone occupancy status. User specified BCVTB inputs written to the controllers included desired configurable points such as high and low limits for SAT and MAT as well as lock-out temperatures for heating, cooling and economizing.

The signals for both economizer damper position and SAT setpoint for five AHU's were gathered from BACnet controllers into BCVTB and from BCVTB into EnergyPlus. The BCVTB model was set up to produce real-time plots of controller signals, system temperatures and various other outputs during simulations for use in a first level analysis of results.

Post simulation data was gathered from both a BCVTB data file including the BACnet signals read from the controllers as well as comma separated value (.csv) files including output variables from the EnergyPlus simulation.

Time for development and execution of co-simulations

The BCVTB model facilitated control of five AHUs. Over 100 EnergyPlus and BCVTB supplied parameters and variables were communicated to three BACnet devices which produced ten signals required to control SAT and economizer damper position for the five units. Each signal required manual connection using the BCVTB graphical user interface. In total an estimated additional fifty hours of time was required to produce a functional BCVTB model.

Time for completion of a simulation varied based on the time step and run period specified in the energy model. Using a desktop PC with twelve gigabytes of RAM, a run period of one month duration using a fifteen minute timestep required between sixteen and eighteen hours of actual time. A single day could be executed in roughly twenty minutes. Simulations of lengthy periods, (greater than a few days), appeared to be subjected to a decreasing completion rate as the experiment progressed. For instance, making calculated predictions for simulation completion using BCVTB actual to simulated time clock could reliably be made for these shorter simulations, but not for lengthier (one month) simulations unless the calculation for completion time was made towards the end of the simulation. If the simulation exceeded a few days, eventually the rate of simulation completion decreased. With multiple controllers in the loop, simulations beyond one month were not possible. The simulation would appear to significantly slow prior to reporting errors with an application crash. In contrast, stand-alone EnergyPlus simulations of similar timestep and run periods may execute in a number of seconds.

The quantity of controllers in the loop as well as the kind of hardware used in the controllers apparently also has an effect on simulation time. Simulations using only the

VLCA-1688 which operates using BACnet IP directly and has a more advanced processor than its VLC predecessors execute somewhat faster. A full year simulation using only the VLCA-1688 to control one unit and a single variable in the simulation can execute in approximately one day [28]. Simulations using much finer timesteps using the model in this previous research took substantially longer for completion. An annual simulation using one minute timesteps took approximately nine days to execute.

3.4.3 Programming of key variables

Programming was completed using the native controller programming software called Envision for BACtalk. This program includes an extension for Microsoft Visio which allows the DDC programmer to use visual logic to design control loops and sequences. Custom DDC programming was created as part of the modeling effort. The basic programming necessary to control a single air handling unit was duplicated and modified to function as additional independent control loops where multiple units are controlled from a single controller. A screenshot of a portion of a control loop is shown in visual logic format in Figure 3.14.

The programming used in co-simulations for this study differ in some respects from the programming used in the actual control network for the physical HVAC system. One key difference is that these control loops are designed to directly produce a desired SAT as a signal for use in the co-simulation instead of producing position signals for heating or cooling coil valve positions. EnergyPlus does not currently support control of AHU coil valve position using an external interface such as BCVTB, whereas desired SAT may be controlled in this fashion.

Development of customized logic for this project was necessary for this and reasons already mentioned. Addition of a second AHU control loop to a particular controller requires relatively simple but significant changes to the cloned logic. Each component of the loop must be uniquely identified. For instance, each block of control logic added using the visual logic program must possess a unique identification number. Furthermore, every binary and

analog value associated with the various control blocks must be also be unique and within certain limitations stipulated in the programming literature of the particular controllers [1]. The decision to share logic for AHU control loops on a couple of the test controllers was necessary because the networking equipment available for the study could handle a limited number of controllers and the number of controllers available was also limited.

Developing customized logic for this project allowed for study of the usefulness of co-simulation as a tool to test controller programming and control sequences. Through an iterative process changes to controller programming were made to develop a fully functional model and to make further improvements to achieve specific goals. Co-simulation was performed to analyze results of the changes. BCVTB's ability to track and display simulation results in real time was utilized as a first level analysis as simulations progressed and after simulation completion. Examples of typical plots configured for auto-generation during co-simulation are included in Figures 3.9 and 3.10. Some details for the situation producing these results follows, but several more plots generated using post-simulation data are included in later sections. The heating setpoint used in the simulation producing Figure 3.9 was 76° F (24.4° C) with a setback to 72° F (22.2° C) .

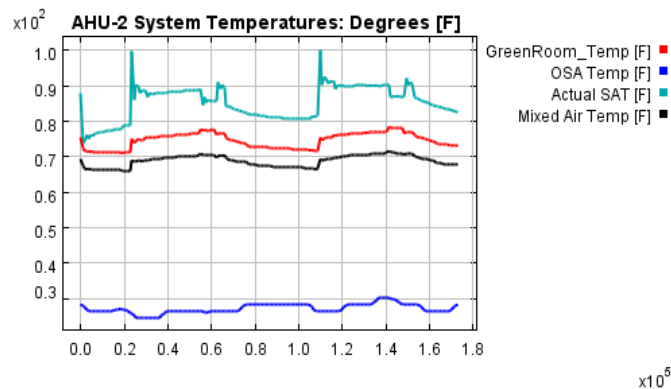


Figure 3.9: Example real time simulation output plot generated by BCVTB showing AHU-2 system temperatures for case B-1.1. Time is along the axis of abscissas displayed in $(s) \cdot 10^5$. The simulation run period was January 22-24 and only data from the first two simulated days are shown. Temperature displayed along the ordinate is in $T \cdot 10^2$. Choice of temperature scale for real time co-simulation output was in °F. SI units are used for duration of this paper.

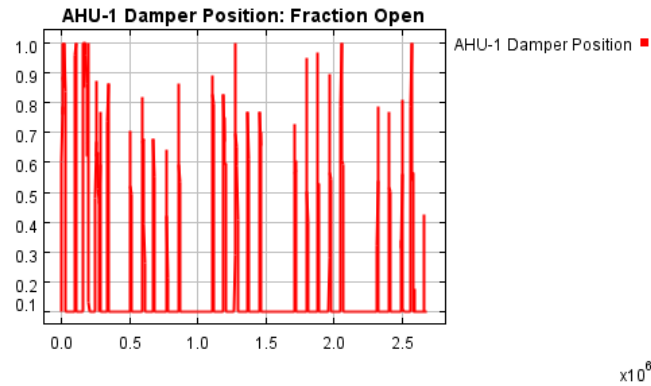


Figure 3.10: Example real time simulation output plot generated by BCVTB showing AHU-1 economizer damper position for a typical co-simulation. Time for the entire month of June is along the axis of abscissas, displayed in $(s) \cdot 10^6$.

Reviewing real time simulation output allowed for relatively quick informed changes between cases, especially in developmental cases where results were initially undesirable.

Supply air temperature (SAT) in heating mode

Control of SAT was designed such that the signal could toggle between a desired heating or cooling temperature depending on current mode of operation. Mode of operation, whether heating or cooling, was determined by a comparison of both outdoor air temperature and heating and cooling signals as derived from two separate proportional-integral (PI) control blocks. This method is depicted in the illustration shown in Figure 3.11. The heating and cooling signals are converted to a desired heating or cooling output temperature by additional logic. Heat or cool mode is determined by cooling mode enable conditions shown in the figure. The resulting output T_{SASP} is the selection of either desired heating or cooling temperature depending on the mode. Thus the SAT is largely determined by PI control. Each signal PI block compares the setpoint (SP) for heating or cooling with the feedback input (FB) or current space temperature. PI output is adjusted in an attempt to get the FB to match the SP .

An ideal PI controller produces a control signal by Eq. (3.1):

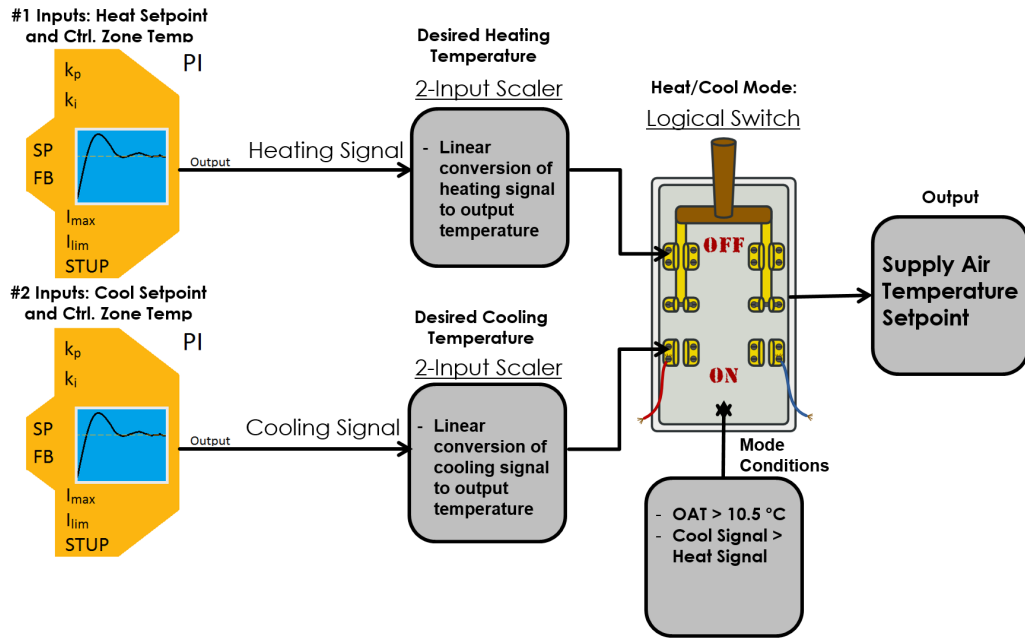


Figure 3.11: Illustration of programming for control of SAT.

$$u(t) = k_p \left[e(t) + \frac{1}{T_i} \int_0^t e(\tau) d\tau \right]. \quad (3.1)$$

In the PI controller the control signal $u(t)$ includes both a proportional and integral component. The proportional component $k_p e(t)$ produces the portion of the output proportional to the control error $e(t)$ which is the difference between FB and SP . The constant k_p is the proportional gain [9], [1]. The integral component is given by Eq. (3.2):

$$I_{out} = k_i \int_0^t e(\tau) d\tau \quad (3.2)$$

where the integral gain k_i is $k_p \left(\frac{1}{T_i} \right)$, and k_p , k_i and T_i are all parameters adjusted as tuning constants by the programmer. The purpose of the integral component is to increase the rate of movement towards the SP and reduce steady-state error. The error term in Eq. (3.2), $e(\tau)$, is the instantaneous error and is summed over time yielding an accumulated offset which is multiplied by k_i and added to $u(t)$.

Alerton visual logic controllers (VLCs) and advanced visual logic controllers (VLCAs)

have options for PI control according to the following equation:

$$u(t) = P + I + 50 \quad (3.3)$$

where P is the proportional component, $k_p e(t)$, and the integral component I is defined by the following relations:

$$I = I_{prev} + I_{inc} \quad (3.4)$$

$$I_{inc} = e(t) \left(\frac{k_i}{60} \right). \quad (3.5)$$

I_{prev} is I from the most recent calculation and additional parameters required are a limit for I called I_{lim} as well as a limit for I_{inc} which is limited to a maximum of $\frac{I_{max}}{60}$. The parameters I_{lim} and I_{max} are also selected by the programmer.

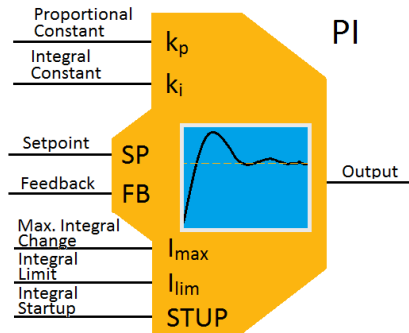


Figure 3.12: Inputs and outputs of Alerton PI block

Figure 3.12 shows inputs and outputs for an Alerton PI block.

The challenge involved in controlling zonal temperatures of control and slave zones connected to five CAV AHUs each supplying conditioned air to multiple spaces via no reheat air terminals is demonstrated via two milestone cases B-1 and B-2. Case B-1 uses initial guesses for appropriate PI tuning parameters and also specifies identical heating setpoints for control and slave zones connected to each AHU. Control of SAT for each AHU was modified between full month cases B-1 and B-2 by smaller iterative subcases B-1.1 through B-1.4 with modifications to PI block parameters for all four cases. Additional changes to

Table 3.5: Comparison of PI and scaling parameters selected for AHU-3 only for iterative sub-cases B-1.1 through B-1.4. Units of temperature are °C.

AHU-3	B-1.1	B-1.2	B-1.3	B-1.4
<i>PI Block</i>				
k_{p1}	0.4	0.4	0.4	0.4
k_{p2}	0.4	12.0	6.0	5.0
k_i	1.0	1.0	1.0	1.0
I_{max}	2.2	2.2	2.2	2.2
I_{lim}	50.0	50.0	50.0	50.0
$STUP$	30.0	30.0	30.0	30.0
<i>2-IN Scaler</i>				
T_{SAL1}	20.6	20.6	20.6	22.2
T_{SAL2}	20.6	20.6	24.4	25.6
T_{SAH}	37.8	37.8	37.8	37.8

the loop handling determination of desired heating temperature to be used as output for SAT setpoint (T_{SASP}) in heating mode were made between a couple of cases and results from these changes are also explained in this section. Through trial and error responses in system behavior to control changes were studied between sub-cases. Case B-2 applies a best guess for PI parameters based on inferences developed by studying results of the sub-cases. Case B-2 applies an increase in heating temperature setpoint (T_{HSP}) from 22.2 to 25.6° C in an attempt to force slave zones up to a T_{HSP} of 22.2° C. It also applies the additional change mentioned to the desired heating SAT control loop for a step increase in the SAT low limit under certain conditions. These changes and related conditions are further explained throughout the following results.

Subcases B-1.1 through B-1.4 selected the three day run period from Jan. 22-24. Previous testing revealed this to be a troublesome period resulting in several hours of unmet heating setpoint. Values of parameters used in control of AHU-3 between sub-cases are shown in Table 3.5. Examples of changes to parameters between simulations are increasing the value of k_i for the heating signal loop in an attempt to increase the rate at which FB reaches the desired SP and increasing the value for T_{SAL2} used in step mode. In cases where results in FB signal showed excessive overshoot, PI gain constants were generally reduced, especially the value for k_p . I_{max} is another parameter that can be adjusted to cap the rate of change of I to alter the responsiveness of the FB . Selections for I_{max} for various control loops

Table 3.6: Comparison of PI and scaling parameters selected for all AHUs for case B-1. Units of temperature are °C.

B-1	AHU-1	AHU-2	AHU-3	AHU-4	AHU-5
<i>PI Block</i>					
k_{p1}	12.0	12.0	12.0	12.0	12.0
k_{p2}	12.0	12.0	12.0	12.0	12.0
k_i	1.0	1.0	1.0	1.0	1.0
I_{max}	3.0	3.0	3.0	3.0	3.0
I_{lim}	50.0	50.0	50.0	50.0	50.0
$STUP$	30.0	30.0	30.0	30.0	30.0
<i>2-IN Scaler</i>					
T_{SAL1}	20.6	21.7	20.6	21.7	20.6
T_{SAL2}	20.6	21.7	20.6	21.7	20.6
T_{SAH}	32.8	32.8	32.8	32.8	32.8

Table 3.7: Comparison of PI and scaling parameters selected for all AHUs for case B-2. Units of temperature are °C.

B-2	AHU-1	AHU-2	AHU-3	AHU-4	AHU-5
<i>PI Block</i>					
k_{p1}	0.4	0.4	0.4	0.4	0.4
k_{p2}	6.0	8.0	5.0	4.0	5.0
k_i	1.0	1.2	1.0	1.2	1.0
I_{max}	2.0	2.7	2.2	2.7	2.2
I_{lim}	50.0	50.0	50.0	50.0	50.0
$STUP$	30.0	30.0	30.0	30.0	30.0
<i>2-IN Scaler</i>					
T_{SAL1}	23.9	25.0	23.3	23.9	23.3
T_{SAL2}	29.4	31.1	26.1	29.4	26.1
T_{SAH}	37.8	37.8	37.8	37.8	37.8

used in case B-2 are shown in Table 3.7. A comparison of the parameter values chosen to produce simulation results for cases B-1 and B-2 can be made by reviewing Tables 3.6 and 3.7, respectively.

Control of actual SAT, (T_{SA}), involves use of a two-input ($2 - IN$) scaling block which ultimately produces the setpoint T_{SASP} . The block uses input which establishes the scaling relationship by which the heating signal from the heating PI block is converted to a desired heating temperature. The scale is created using the high and low heating setpoint limits, T_{SAH} and T_{SAL} . T_{SASP} in heating mode is determined by taking the heating signal as an input, converting it to a percentage of a full heating signal and linearly determining a point between T_{SAL} and T_{SAH} to output as the setpoint.

An illustration of the $2 - IN$ scaler producing T_{SASP} is shown in Figure 3.13. Switching logic was added to the inputs for OUT1 and OUT2 to produce a step increase in the lower end of the scale when zone heating setpoint (T_{HSP}) is greater than the control zone temperature (T_{CZ}). The step mode also included the option to toggle to a new selection for PI parameters k_p and k_i when the condition for step mode was satisfied. Allowing the $T_{HSP} > T_{CZ}$ condition to change the value of a PI parameter during co-simulation was employed in cases B-1.2 through B-1.4 as well as B-2 for the value of k_p only. Setpoints for T_{SAL} and T_{SAH} , as well as input parameters for heating signal PI block were altered in an iterative fashion by reviewing simulation output plots similar to those shown previously in Figures 3.9 and 3.10 in an attempt to determine which parameter changes would produce desired effects.

Cases B-1.2 through B-1.4 included a step mode based on the $T_{HSP} > T_{CZ}$ condition for the value of k_p . Case B-1.3 differed from previous cases by inclusion of the step mode to toggle between T_{SAL1} and T_{SAL2} when the same condition was met. Case B-1.4 included more customized changes to PI parameters for control of each individual AHU. The purpose of these changes was to drive each T_{CZ} and T_{SZ} towards its T_{HSP} for as much of the run period as possible. Comparing results from case B-1.4 with cases B-1.1 through B-1.3 helped determine settings for an improved full month simulation, case B-2, with custom parameter

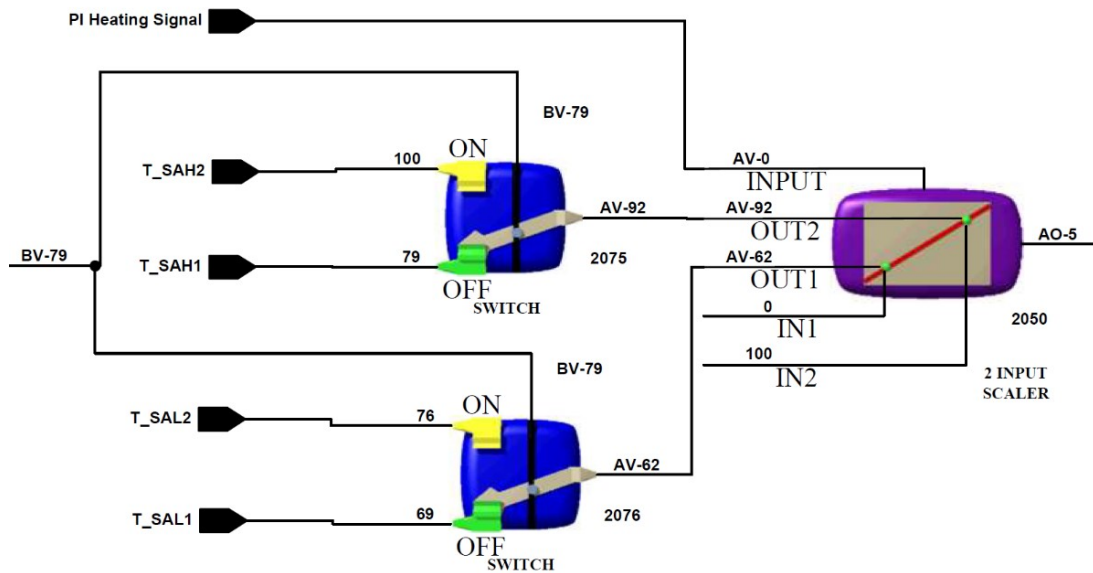


Figure 3.13: 2 – IN scaler block used to produce T_{SASP} along with input logic designed to produce step increase in both T_{SAH} and T_{SAL} at times when (T_{HSP}) is greater than the control zone temperature (T_{CZ}).

settings for control of each AHU.

Economizer damper and cooling mode

Three separate economizer control schemes were attempted and are highlighted in cases A-1 through A-4 which all used Model Q. The method and process of making changes to economizer control was similar to the means described for changing control of SAT in heating mode. Parameter and control loop changes were made between cases. Table 3.8 includes a list of major differences between these cases. SAT in cooling mode was allowed to modulate between a high temperature (T_{SAH}) and a low temperature (T_{SAL}).

A list of reference names for symbols indicated in Table 3.8 is included in Table 3.9.

Economizer damper position was controlled by a signal generated by one of three basic scenarios. Cases A-1 and A-3 both use a 2 – IN scaler block which takes the signal output from the PI block belonging to the cooling loop (see Figure 3.14) as its input. The PI cooling signal can range anywhere between zero and 100. Control in cases A-1 and A-3

Table 3.8: List of changes made between cases A-1 and A-4 to control economizer damper modulation. “NR” used to indicate that a particular parameter is not required in the logic.

Case	T_{SAH}	$T_{MAT}; L$	$T_{MAT}; H$	Economizing Signal
A-1	19.9	14.4	20.0	2- IN scaler based on cooling signal
A-2	19.9	14.4	20.0	2- IN scaler based on cooling signal, different enable conditions
A-3	18.3	14.4	20.0	2- IN scaler based on cooling Signal
A-4	18.3	NR	NR	PI, control MAT to T_{SASP}

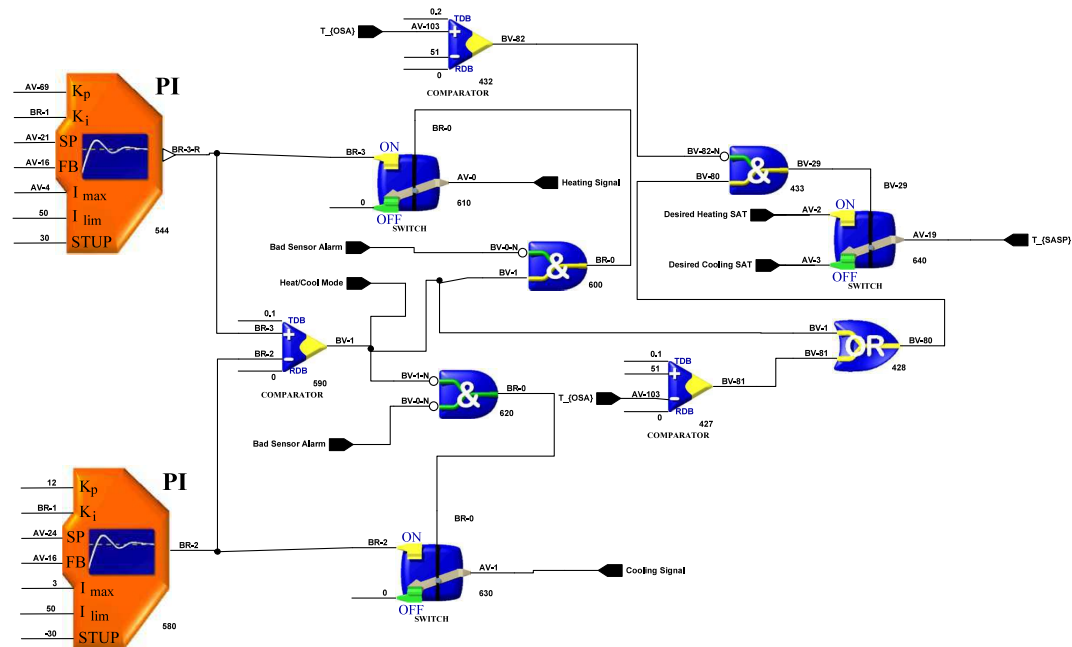


Figure 3.14: View of partial screenshot showing portion of logic for SAT control as well as PI blocks used for generating heating and cooling signals.

was patterned after the default building control for economizing. Default control allowed the cooling signal to produce economizer modulation when the outside temperature was less than the economizer lock-out temperature. If the enable condition was not met, the signal would switch to the economizer low limit of 10%. If any cooling signal above 3% occurred and enable conditions were satisfied, then the initial output would be 100%. However, this output was further limited by the following condition. The output signal was scaled based on the range of MAT between the MAT low limit ($T_{MAT;L}$) and high limit ($T_{MAT;H}$). This produced further modulation between zero and 100% according to these MAT limit parameters by an additional $2 - IN$ scaler. The limiting effect of this scaling condition favored the low end of the specified MAT range. For example, if the current MAT is the $T_{MAT;L}$, the result would be a signal of zero. Linear modulation up to a high point of 100 for a MAT greater or equal than $T_{MAT;H}$ is possible so long as the enable conditions are met.

Table 3.9: Full description of key temperatures indicated as abbreviated temperature symbols used in Table 3.8. Identical symbols used in subsequent sections have the same meaning.

Symbol	Reference meaning
T_{SAH}	A high limit for AHU supply temperature in a particular mode
$T_{MAT;L}$	AHU mixed air temperature low limit
$T_{MAT;H}$	AHU mixed air temperature high limit

Case A-2 used the same PI cooling control signal but differed from these other cases by allowing for linear modulation of the initial economizing output signal for a range of cooling signals between zero and 30% instead of zero and 3%. In this case any cooling signal above 30% results in an initial economizer output signal of 100%. Additionally another enabling condition was applied which required OAT to be less than RAT. The goal of this was to improve economizer operation between cases A-1 and A-2.

Case A-4 used a different control method altogether. Instead of using the cooling loop signal as the basis for economizer control, an additional PI block was added which compared T_{MAT} to T_{SASP} . The idea was to control damper modulation to match T_{MAT} to the T_{SASP} .

An additional modulation to this signal was not added like that used in the default control. Instead, simple constraints for economizer operation were added ensuring current space temperature exceeds the heating setpoint and outside air temperature is within a range from 14.4 to 22.2 °C. Outside temperature also had to be less than RAT. Slight changes were made to parameters such as the high limit for T_{SAH} in cooling mode and $T_{MAT}; L$. These changes are shown in Table 3.8. Cases A-3 and A-4 also used a lower T_{SAH} than A-1 and A-2.

3.5 Results

In this section results from January and August cases are treated. January cases focused on developing SAT control to meet zone heating setpoints, while August cases focus on logic for appropriate economizer function. The various cases are compared and contrasted by criteria including how often heating setpoint is met, changes in energy usage, and visual inspection of signal responses.

3.5.1 SAT control in heating mode for January cases

Initial co-simulations for January cases used Model Q. Results for January simulations with this model consistently showed hours of unmet heating setpoint regardless of changes to programming. This was especially true for control zones CZ-1 and CZ-2 for AHU-1 and AHU-2 respectively. Simulation results for a previous case C-1 which used Model Q, for the one week period of Jan. 18-24, are shown in Figure 3.15. Abbreviated temperature symbols included in the figure legend are referenced with their respective full names for convenience in Table 3.10.

Figure 3.15 highlights a comparison of signals for AHU-2 for a three day run period late in January. The figure shows variation in T_{HSP} from 22.2° C, the occupied heating setpoint, down to 20° C, the setback temperature for periods of unoccupancy. The controller

Table 3.10: Full names referenced to abbreviated temperature symbols used in Figure 3.15. Identical symbols used in subsequent figures have the same meaning.

Symbol	Reference meaning
T_{SA}	AHU supply air temperature
T_{SASP}	Supply air temperature setpoint
T_{CZ}	Space air temperature of the AHU control zone
T_{OA}	Outside air temperature
T_{HSP}	Space heating setpoint

attempts to modulate T_{SA} high enough to cause T_{CZ} to match T_{HSP} . The figure highlights the transition from a period where T_{SASP} initially results in a similar response, T_{SA} , to a period where significant divergence occurs. This situation is contrasted by case B-2 using Model R. Figure 3.16 shows AHU-2 signals for the same run period with no apparent discrepancy between T_{SA} and T_{SASP} . The problem was found to be insufficient capacity available in the heating plant loop for Model Q.

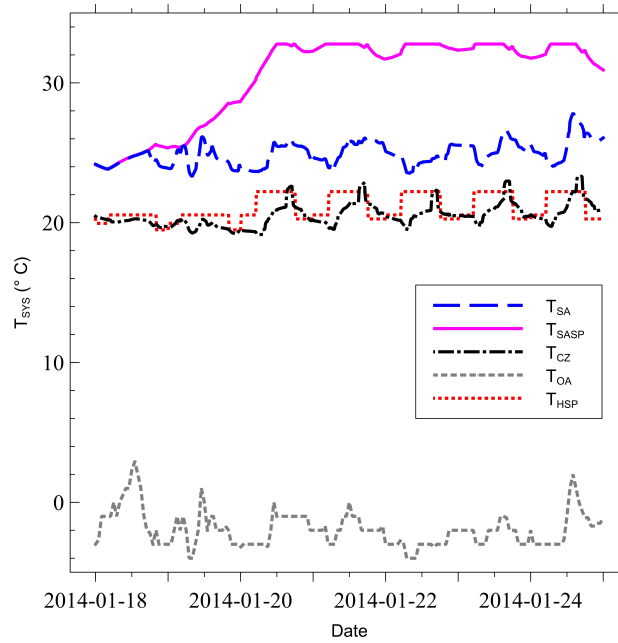


Figure 3.15: AHU-2 system temperatures contrasting T_{CZ} response T_{SA} with T_{SASP} for case C-1 using Model Q and simulation run period Jan. 18-24.

Subsequent January simulations were run using Model R. This model employed a district heating plant loop instead of a natural gas boiler. Figure 3.17 shows the SAT signals for Jan. 18-24 for case B-1 and can be compared with the control zone response, T_{CZ} , for the

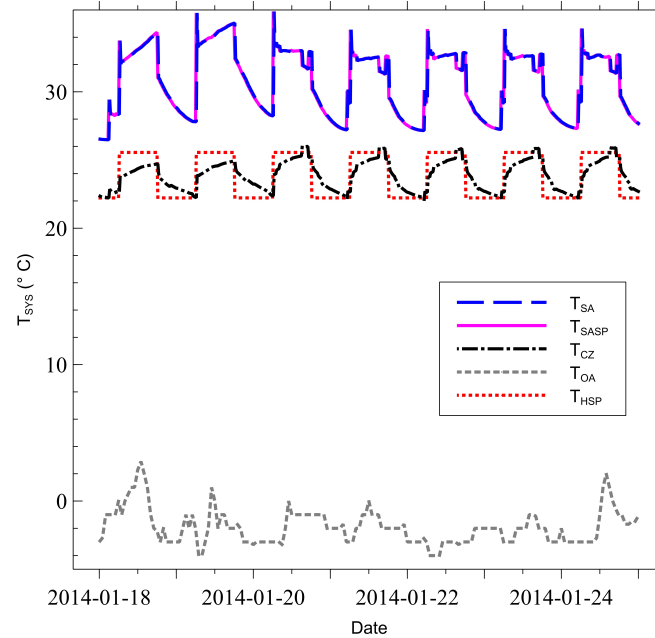


Figure 3.16: AHU-2 system temperatures contrasting T_{CZ} response T_{SA} with T_{SASP} for case B-2 using Model R and simulation run period Jan. 18-24.

same case and period in Figure 3.19. Results and reference information for cases B-1 and B-2 including heating temperature setpoints (T_{HSP}) for all control and slave zones are shown in Table 3.11. Several slave zones in case B-1 have hours where T_{HSP} is not met. Figure 3.19 indicates close correlation between T_{CZ} and T_{HSP} for control zone CZ-3. Slave zones SZ-3.1 through SZ-3.9 attached to this CZ-3 have especially high amounts of unmet hours for T_{HSP} . Seven of the nine slave zones have well above 100 unmet hours for the month in case B-1.

Table 3.11 also displays a comparison of the time heating setpoint is not met (t_{HSPX}) for both control and slave zones during occupied hours in January. Adjusting the control zone occupancy temperature and applying custom improvements via insights gained from sub-cases B-1.1 through B-1.4 to each AHU's control logic shows considerable improvement in unmet hour reduction between cases B-1 and B-2 where unmet hours were reduced by 91%. Changes to control loop parameters between these cases are included in Table 3.6 and Table 3.7. Figures 3.17 and 3.19 may be contrasted with Figures 3.18 and 3.20, highlighting

Table 3.11: Comparison of (t_{HSPX}) hrs. during occupied times for each control (CZ) and (SZ) for cases B-1 and B-2 during January. Temperature units are in °C.

Case		B-1		B-2	
Model		R		R	
Comparison Data	Abbrev.	T_{HSP}	t_{HSPX}	T_{HSP}	t_{HSPX}
<i>AHU-1</i>					
<i>Control Zone</i>					
129_Auditorium	CZ-1	22.2	0.5	25.6	5.8
<i>Slave Zones</i>					
B17_Orchestra_Pit	SZ-1.1	22.2	0.0	22.2	0.0
M134_Transformer	SZ-1.2	22.2	296.8	22.2	0.3
M135_Mechanical	SZ-1.3	22.2	333.3	22.2	327.3
S001_Catwalk	SZ-1.4	22.2	239.3	22.2	0.0
<i>AHU-2</i>					
<i>Control Zone</i>					
M116_Green_Room	CZ-2	22.2	0.0	25.6	2.5
<i>Slave Zones</i>					
M119_Men_Dressing	SZ-2.1	22.2	0.0	22.2	0.0
M117_Makeup	SZ-2.2	22.2	2.3	22.2	0.0
M120_Women	SZ-2.3	22.2	0.0	22.2	0.0
M121_Men's	SZ-2.4	22.2	0.8	22.2	0.0
M122_Corridor	SZ-2.5	22.2	0.0	22.2	0.0
M126_WORKSHOP	SZ-2.6	22.2	0.0	22.2	0.0
<i>AHU-3</i>					
<i>Control Zone</i>					
M111_Lobby	CZ-3	22.2	0.0	25.6	2.5
<i>Slave Zones</i>					
M101_Vest	SZ-3.1	22.2	216.5	22.2	0.8
M102_Box_Office	SZ-3.2	22.2	91.5	22.2	0.0
M104_Coat_Room	SZ-3.3	22.2	147.8	22.2	0.0
M106_107_Closet	SZ-3.4	22.2	0.0	22.2	0.0
M108_Men	SZ-3.5	22.2	173.8	22.2	0.0
M109_Women	SZ-3.6	22.2	168.8	22.2	0.0
M112_Entry	SZ-3.7	22.2	297.5	22.2	0.0
M113_Ramp	SZ-3.8	22.2	230.3	22.2	0.0
S213_Vestibule	SZ-3.9	22.2	52.3	22.2	0.0
<i>AHU-4</i>					
<i>Control Zone</i>					
S203-205_Costume	CZ-4	22.2	0.0	25.6	6.8
<i>Slave Zones</i>					
S127_Stairs	SZ-4.1	22.2	164.8	22.2	0.0
S201_Fitting	SZ-4.2	22.2	0.0	22.2	0.0
S202	SZ-4.3	22.2	93.8	22.2	1.3
S206_Storage	SZ-4.4	22.2	640.8	22.2	0.0
<i>AHU-5</i>					
<i>Control Zone</i>					
B7-B9_Storage	CZ-5	22.2	0.0	25.6	3.0
<i>Slave Zones</i>					
B12_Storage	SZ-5.1	22.2	0.0	22.2	0.0
B13_Trap_Room	SZ-5.2	22.2	0.0	22.2	0.0
B14_Storage	SZ-5.3	22.2	0.0	22.2	0.0
B3_Scene_Prop	SZ-5.4	22.2	632.3	22.2	0.0
B4_Corridor	SZ-5.5	22.2	274.8	22.2	0.0
M126_WorkshopB	SZ-5.6	22.2	0.0	22.2	0.0
Total			4,057.3		350.0
Amount Reduced			3,707.3		
Percent Reduction			91.3		

Table 3.12: Time heating setpoint is not met, (t_{HSPX}) in (hrs.), during occupied times for the five control zones for cases B-1.1 through B-1.4 as well as results from B-2 for Jan. 22-24.

Case		B-1.1	B-1.2	B-1.3	B-1.14
Model		R			
Unit information	Symbol	t_{HSPX}			
<i>AHU-1</i>					
129_Auditorium	CZ-1	16.0	9.0	8.0	8.8
<i>AHU-2</i>					
M_116_Green_Room	CZ-2	20.8	12.3	6.5	14.5
<i>AHU-3</i>					
M111_Lobby	CZ-3	8.3	9.8	4.0	0.0
<i>AHU-4</i>					
S203-205_Costume	CZ-4	16.3	8.0	10.3	11.5
<i>AHU-5</i>					
B7-B9_Storage	CZ-5	10.8	6.3	5.5	9.3

the difference in setpoints and responses contributing to improvements in unmet hours for slave zones between cases B-1 and B-2. T_{SASP} signals for case B-2 shown in Figure 3.18 increased in magnitude compared to those from case B-1 shown in Figure 3.17. Magnitude of both T_{HSP} and T_{CZ} also increased between these cases as shown in Figures 3.19 and 3.20.

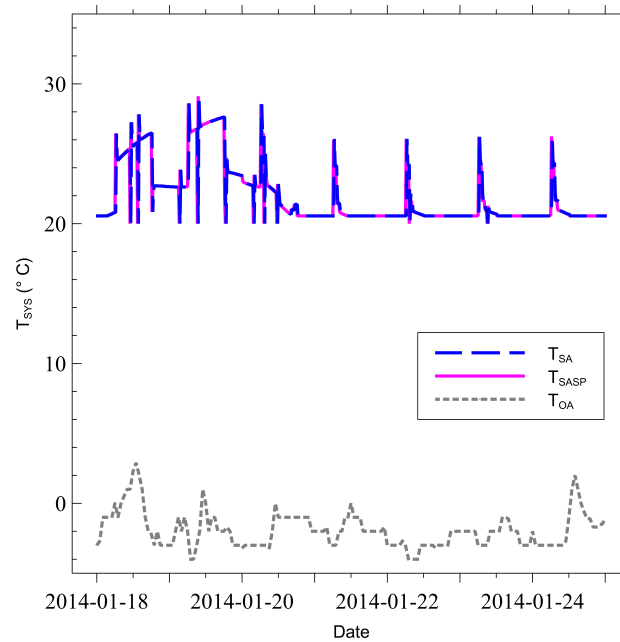


Figure 3.17: AHU-3 system temperatures contrasting T_{CZ} response T_{SA} with T_{SASP} for case B-1 using Model R and simulation run period Jan. 18-24.

Table 3.12 displays time heating setpoint is not met (t_{HSPX}) during occupied hours for the five control zones for sub-cases B-1.1 through B-1.4. Most systems show decrease

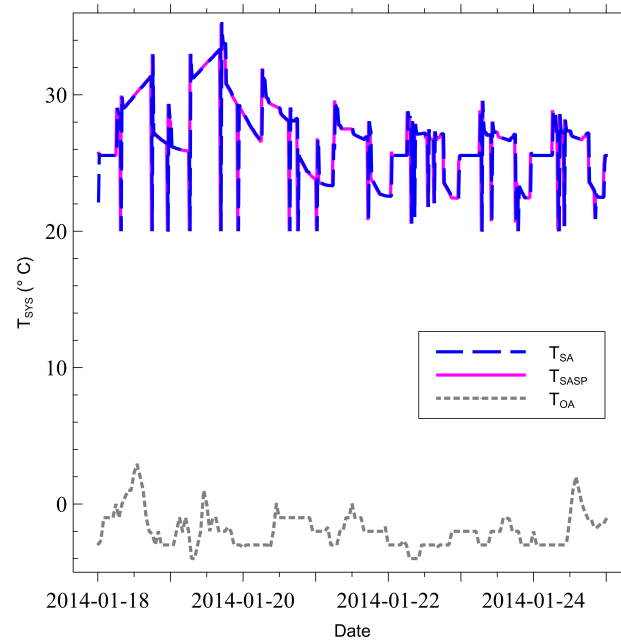


Figure 3.18: AHU-3 system temperatures contrasting T_{CZ} response T_{SA} with T_{SASP} for case B-2 using Model R and simulation run period Jan. 18-24.

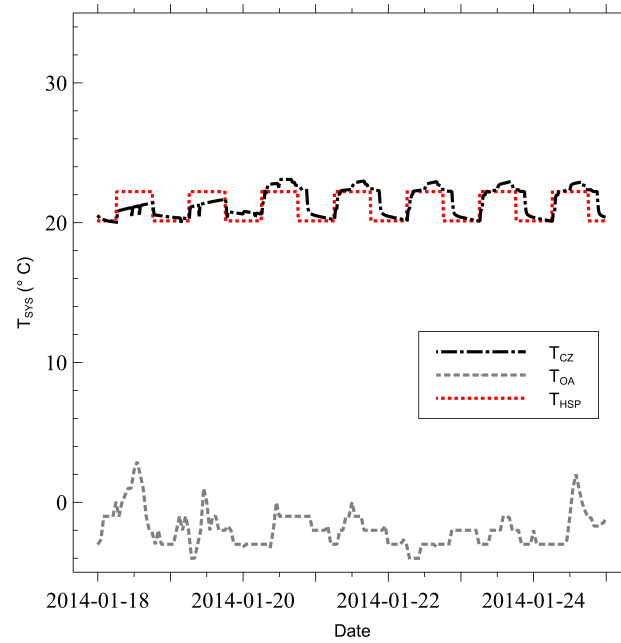


Figure 3.19: AHU-3 system temperatures contrasting T_{CZ} response with T_{HSP} for case B-1 using Model R and simulation run period Jan. 18-24.

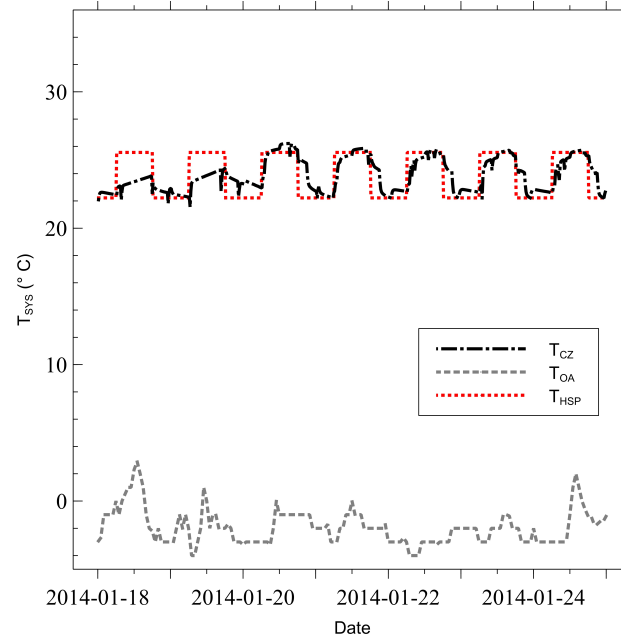


Figure 3.20: AHU-3 system temperatures contrasting T_{CZ} response with T_{HSP} for case B-2 using Model R and simulation run period Jan. 18-24.

in unmet hours between cases B-1.1 and B-1.3, while AHU-3 is the only system showing decrease between cases B-1.3 and B-1.4. Reviewing changes in the selected settings shown in Table 3.5 and the results shown in Table 3.12, insights were developed into choosing the parameters and settings used in case B-2.

Comparisons of control of AHU-3 system temperatures highlighting the response of T_{CZ} with iterative changes to controller logic are shown in Figures 3.21, 3.22, 3.23 and 3.24. The AHU controlled signal T_{SA} is responds to different controller logic between iterations in an attempt to match T_{CZ} to T_{HSP} . In these cases T_{SASP} is purposefully neglected as it is visually identical to T_{SA} . The space setpoint, T_{HSP} experiences periods of setback from 25.6 to 22.2° C from periods of occupancy to unoccupancy. Figure 3.21 shows an under-responsive T_{SA} preventing T_{CZ} from adequately reaching T_{HSP} for about 8 hrs. of the period. Figures 3.22 and 3.23 both show variations of an over-responsive T_{SA} signal. Case B-1.2 resulted in worse performance whereas case B-1.3 reduced unmet hours by half. Figure 3.24 shows a well-tuned response which resulted in zero unmet hours for the run period.

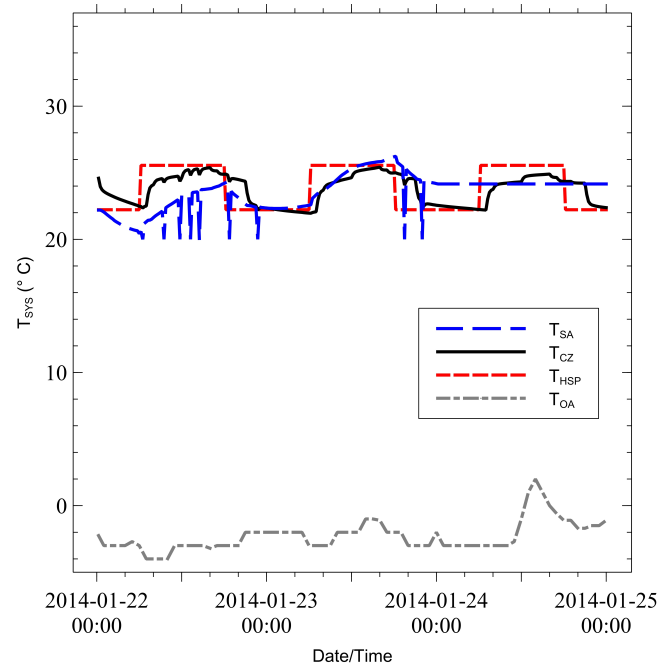


Figure 3.21: AHU-3 system temperatures highlighting T_{CZ} response, T_{SA} , for case B-1.1 using Model R and simulation run period Jan. 22-24.

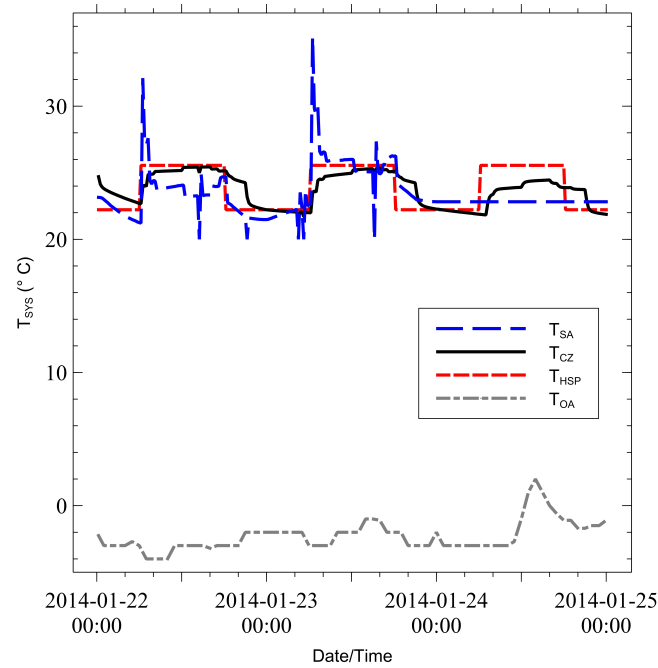


Figure 3.22: AHU-3 system temperatures highlighting T_{CZ} response, T_{SA} , for case B-1.2 using Model R and simulation run period Jan. 22-24.

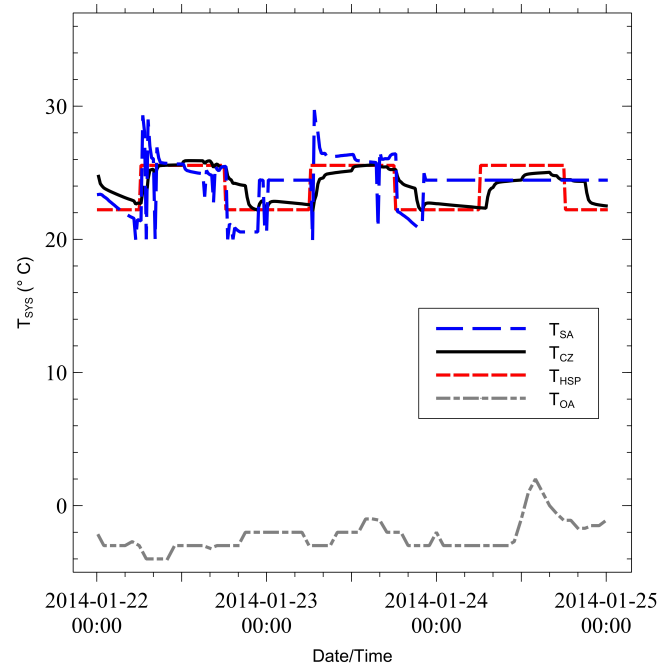


Figure 3.23: AHU-3 system temperatures highlighting T_{CZ} response, T_{SA} , for case B-1.3 using Model R and simulation run period Jan. 22-24.

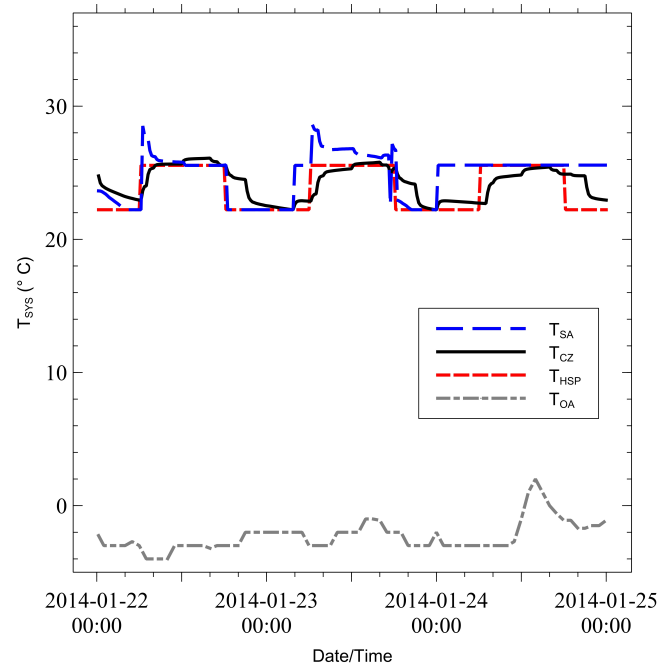


Figure 3.24: AHU-3 system temperatures highlighting a well tuned T_{CZ} response, T_{SA} , for case B-1.4 using Model R and simulation run period Jan. 22-24.

For all cases shown in these results, reduction in unmet hours resulted in increased energy use. Figure 3.25 shows the variation in heating energy used between sub-cases. Results indicated that over the three day period, there was about a 4% decrease in energy use between cases B-1.1 and B-1.2. Figure 3.25 also indicates increases of approximately 10% and 19% from case B-1.1 to cases B-1.3 and B-1.4, respectively. Figure 3.26 shows the increase in total facility energy use between cases B-1 and B-2. Energy increased between these cases by 21 MWh, an increase of approximately 30%.

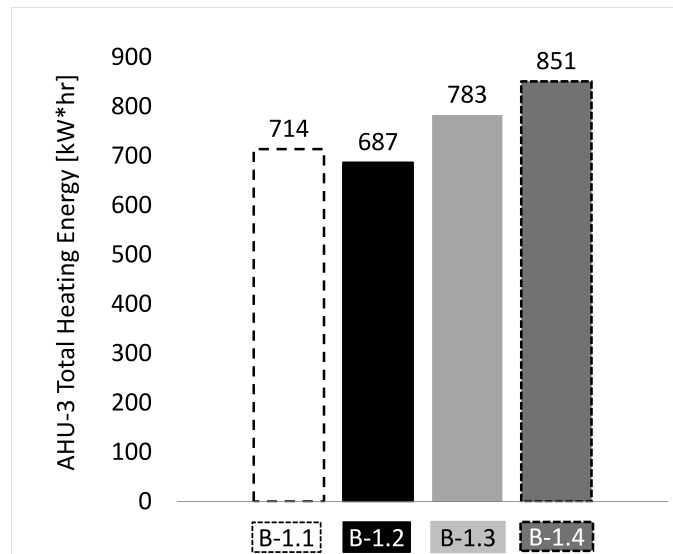


Figure 3.25: Comparison of AHU-3 total heating energy between sub-cases B-1.1 through B-1.4.

3.5.2 Economizer control in august cases

Case A-1 resulted in poor economizer control as shown by the signal graph in Figure 3.27. Figure 3.27 shows economizer damper position in terms of fraction of a fully open position throughout time. The damper position for each AHU is indicated by its respective number shown in the figure legend. Early in the run period AHU-3 damper open fraction increases to the fully open position, and the AHU-4 damper reaches a mostly open (90% of full) condition. The initial responses showing modulation prior to reaching the positions shown in the figure are not visible as the selected timeframe shown begins after simulation

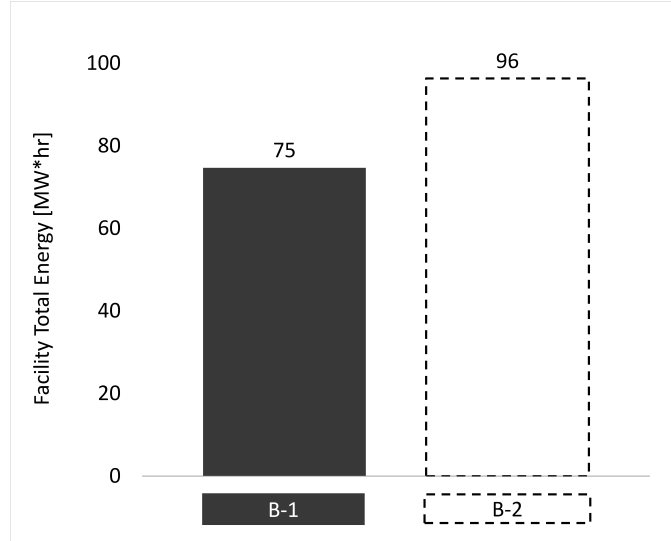


Figure 3.26: Comparison of total facility energy use between cases B-1 and B-2.

onset. Damper position for these units remains constant for the remainder of the run period. Although only one week is shown in the figure, this condition persisted for the whole month of August. Similarly, AHU-1, AHU-2, and AHU-5 showed slight modulation at simulation onset but switched back to and remained at the minimum position for the remainder of the run period.

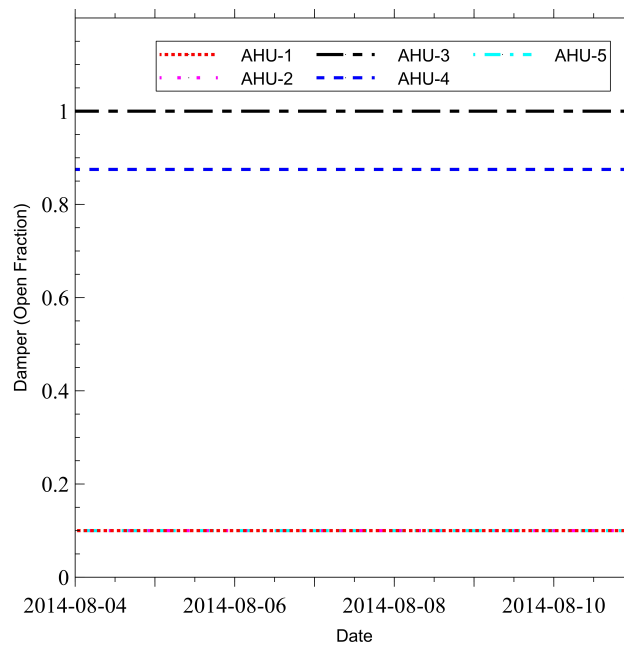


Figure 3.27: Signals for damper open fraction for all AHUs from case A-1.

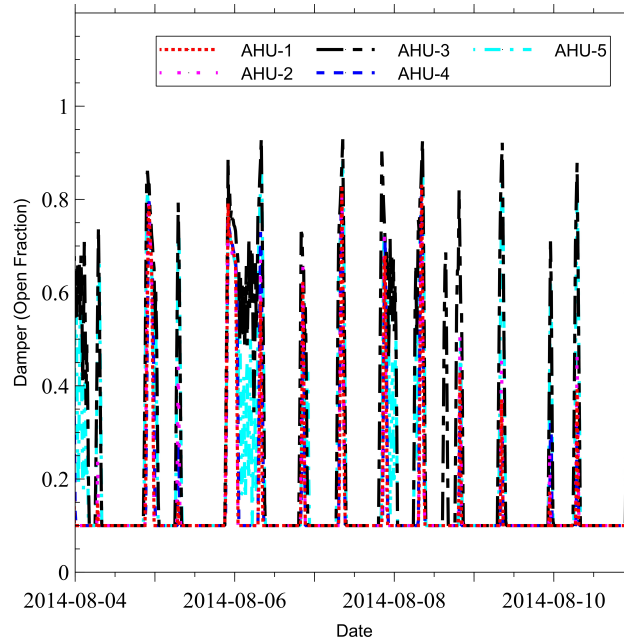


Figure 3.28: Signals for damper open fraction for all AHUs from case A-2.

Apparent improvement is shown for case A-2 in Figure 3.28, where all units modulate mostly at times both early and late in the day throughout the first week in August, which seems like reasonable economizer function. Results from case A-4 are shown in Figure 3.29 where function also seems reasonable but operates somewhat differently. Economizer logic was changed between these examples and less conservative functionality results with additional periods where economizer dampers reach the fully open position in case A-4.

An example of system temperatures from a sample AHU, AHU-3, are shown for case A-1 in Figure 3.30. The signals shown in this figure include a space response T_{CZ} to the air handler SAT, T_{SA} , which is appears constant throughout this period. T_{OA} is included in this view to provide a frame of reference for the other temperatures shown. The cooling setpoint T_{CSP} during occupied times is 23.9°C with a steps up to a maximum point of 26.7°C for periods of unoccupancy. Similar plots at this scale which include T_{OA} for cases A-2 through A-4 appear too similar to make comparisons in signals between cases. Figures 3.31, 3.32 and 3.33 are comparisons of all of these signals except T_{OA} which is excluded in order to show an appropriate scale for comparison. Another similar figure for case A-1 is not included among

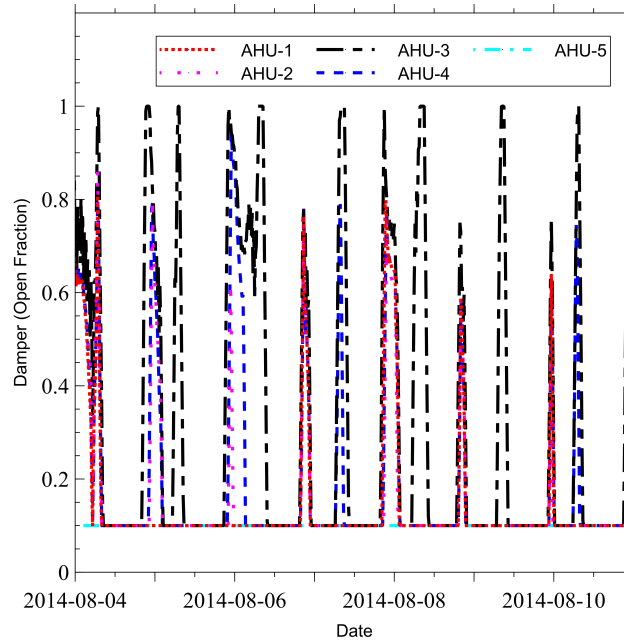


Figure 3.29: Signals for damper open fraction for all AHUs from case A-4.

these results because system temperatures appear to be identical between cases A-1 and A-2. Cooling energy reduces even further when contrasting cases A-2 and A-3. Contrasting Figure 3.31 and Figure 3.32 there are apparent differences in T_{SA} . Figure 3.31 shows a flat signal, while Figure 3.32 has periods of increasing and decreasing T_{SA} at nights where OAT falls below 14.4°C . This is because the controls were designed to lock out heating below 14.4°C which in this case is apparently too high. Although there is some heating energy that is present in both cases this is mostly due to plant energy which is also in operation at these times due to the settings for the plant setpoint managers recorded in Table 3.4. Even though cooling energy is less in case A-3, a net reduction in heating energy due to the higher heating. A similar effect is noticed for certain times for case A-4 as seen in Figure 3.33.

Additional similar figures for other AHUs simulated are not included because the signals for are very similar for all units for a particular case. Varying levels of increases and decreases of cooling energy resulted for changes between cases A-1 through A-4. Table 3.13 indicates the results for cooling energy between these cases. Changes to the logic including the changes to the initial economizing signal range of modulation and the added enabling condition

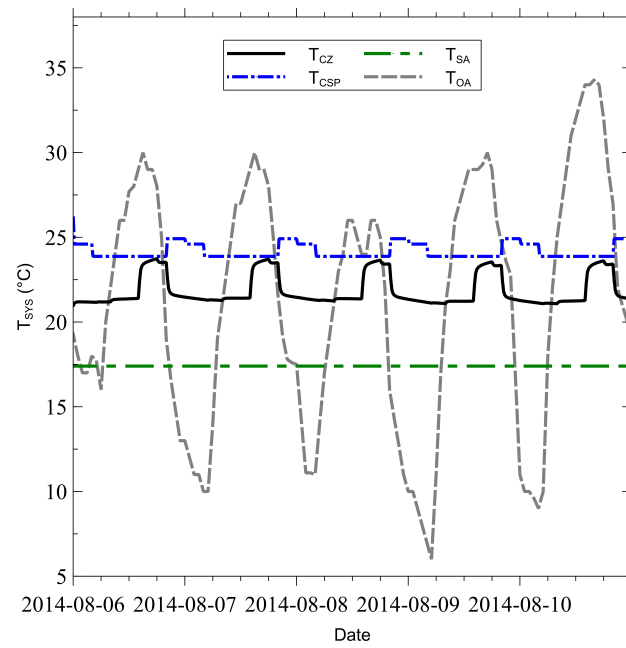


Figure 3.30: AHU-3 system temperatures for case A-1 throughout five day time period from Aug. 6-10.

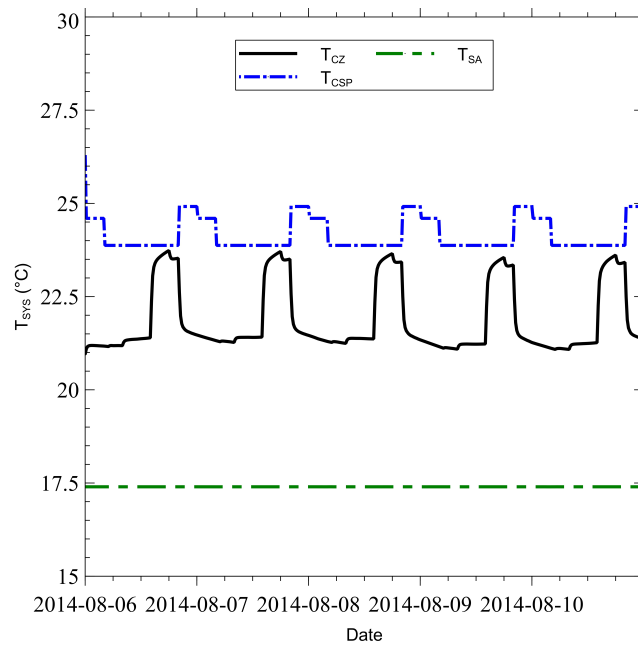


Figure 3.31: AHU-3 system temperatures for case A-2 throughout five day time period from Aug. 6-10.

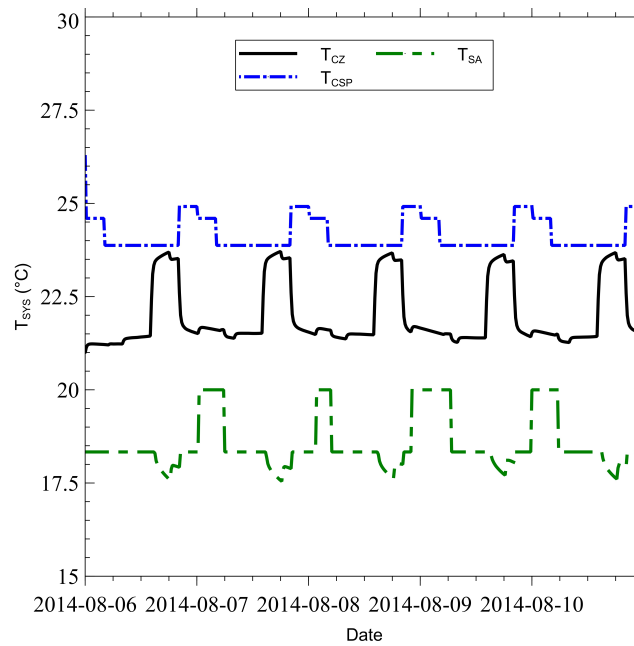


Figure 3.32: AHU-3 system temperatures for case A-3 throughout five day time period from Aug. 6-10.

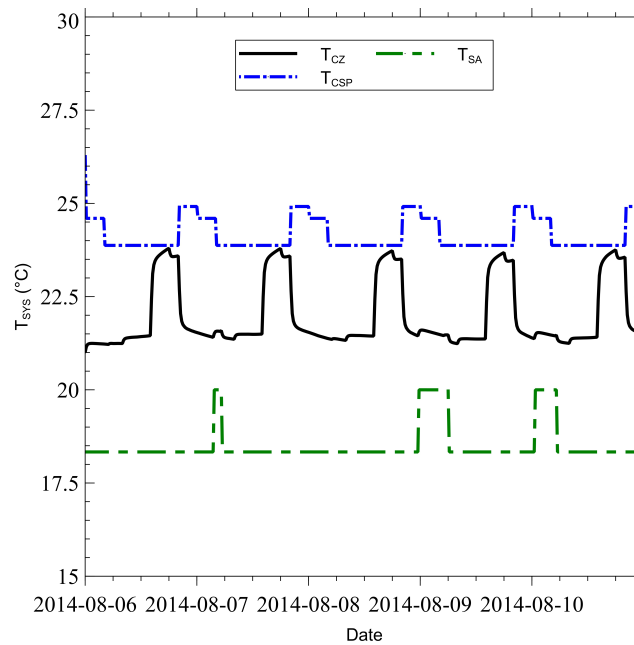


Figure 3.33: AHU-3 system temperatures for case A-4 throughout five day time period from Aug. 6-10.

indicated in Table 3.8 improved behavior of all AHU economizer dampers between cases A-1 and A-2 and resulted in a reduction in cooling energy. The percent change between these and other cases can be contrasted by referring to Figure 3.34 where the largest percent change is between cases A-1 and A-2 where cooling energy reduced by about 5%. Cooling energy increases between cases A-3 and A-4. The parameter selections which caused energy changes between cases are shown in Table 3.8.

Table 3.13: Comparison of cooling energy use (kWh) for cases A-1 through A-4 for the month of August

Case	Cooling Energy
A-1	12,406
A-2	11,847
A-3	11,561
A-4	11,992

An important note here is that A-3 did not result in any significant (above minimum) economizing activity for all AHUs. While not shown in previous plots, A-3 economizing activity for all AHU's was nearly constant at the minimum 10% position for the entire run period.

The only parameter difference between cases A-2 and A-3 is the reduction of T_{SAH} from 19.9 to 18.3° C. Recall T_{SAH} is the high limit of AHU supply air temperature in cooling mode. The reduction of this parameter by 1.6° C even with as little economizing as there was in case A-3, resulted in a net decrease in cooling energy when comparing either cases A-2 or A-4. It is suspected that this effect may result in further reduction of cooling energy if the same condition were applied to case A-2 and co-simulation performed. This possibility cannot be verified at this time as this exact situation was not tested. However, it is supported by the fact that there was a significant reduction in cooling energy between cases A-1 and A-2. Case A-1 uses the same logic as A-2 and only differs with respect to a single parameter change indicated in Table 3.8. Nonetheless testing would be required to determine whether this suspicion would be upheld by simulated results.

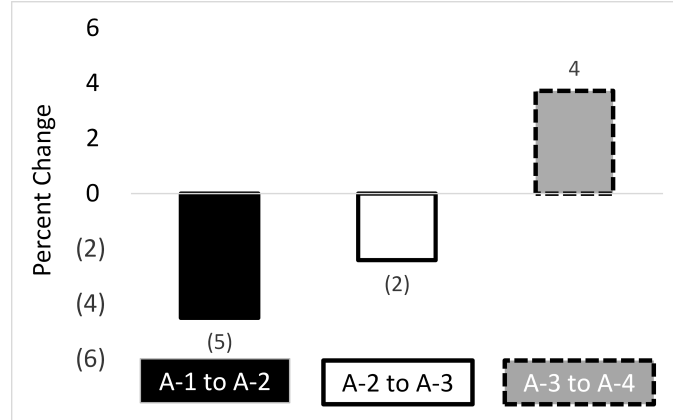


Figure 3.34: Percent change, increases and (decreases), in cooling energy use between selected cases.

3.6 Discussion

In general these results demonstrate that iterative changes to DDC logic may be tested in a relatively automated fashion using co-simulation. An energy model can be used in developing new control logic. Inferences may be gleaned through both surface level results as well as more in depth analysis using simulation output files. Through an iterative process improvements in parameter selections and control loop logic may be made. Further discussion of simulation results follows in the remainder of this section.

3.6.1 January cases

January cases provide examples of how a control of a system may be improved through co-simulation. Because the units are all constant volume systems with no reheat air terminals, T_{SZ} of each slave zone depends on a high enough control zone T_{HSP} in order to reach its heating setpoint. If T_{HSP} is sufficiently high, unmet hours for other zones attached to the air loop will be reduced to zero. This is demonstrated by the large reduction in unmet hours from cases B-1 to B-2 where hours of unmet heating setpoint (t_{HSPX}) was reduced by 91%. Nonetheless, reduction in unmet hours using this technique result in up to 30% increase in energy use.

Proper tuning of PI and in some cases proportional integral derivative (PID) parameters is critical for correct system response. Examples of tuning effects on system response are apparent in results shown in figures in the results presented earlier. Co-simulation is a platform by which currently these settings may be determined through a trial and error approach. As demonstrated by sub-iterative cases B-1.1 through B-1.4, co-simulation improvements in this study have been accomplished by this approach. Thus changes can be made, and the effects of these changes may be studied through co-simulation. Several studies have investigated ways into more automatic means optimizing of HVAC performance through auto-tuning PI or PID parameters as well use of various optimization algorithms which solve specific optimization problems. In [23], [20] and [18] advanced methods of feedback tuning PI and PID controllers used for HVAC applications are discussed. In [27], [17] and [26] use of optimization algorithms for improvement of HVAC control is demonstrated and discussed. These methods show considerable potential for making improvements to system function. The possibility of using appropriate automated optimization of parameters or variables in co-simulation is a topic for future studies.

Actual changes to a control loop such as the step increase to T_{SAL} when $T_{HSP} > T_{CZ}$ in sub-iterations between cases B-1 and B-2 is an additional method which was investigated as a means to increase control responsiveness. In some cases this seemed to contribute to reduction in unmet hours as was demonstrated by the change between sub-iterative cases B-1.2 and B-1.3 where the result was a reduction in unmet hours for all control zones except for CZ-4 as shown in Table 3.12. Here the most significant reductions are shown for both CZ-2 and CZ-3 which are the control zones for the second and third largest AHUs. While this was an idea that proved useful towards improving simulated system response, care must be taken when making changes to control of actual equipment. If a controller drives system response too aggressively, equipment and property may be damaged. As always, equipment manufacturers guidelines must be followed. Thus, it is recommended to implement changes studied using co-simulation gradually when transitioning to control of actual equipment.

Benefits of co-simulation in isolating various scenarios for control purposes especially relating to the challenge of controlling CAV systems are apparent if the results from EnergyPlus stand-alone simulations are contrasted versus simulations executed with real controllers within the loop. Best cases derived with moderate effort in EnergyPlus such as those demonstrated by cases R-1 and R-2 each had several zones with high t_{HSPX} . While this set of results was not covered in detail in earlier sections, a summarized overview is that t_{HSPX} for twenty zones were significantly above zero in the best of the two scenarios (R-1), where nine of these zones had t_{HSPX} each greater than 500 hours. Efforts to produce improvements for in t_{HSPX} using co-simulation resulted in controller logic capable of reasonably regulating space temperatures and resulted in a control solution from which results can be demonstrated that reflect the control goal. This is especially apparent in January cases for reasons explained earlier.

3.6.2 August cases

August cases demonstrate a way that economizer control may be tested using co-simulation. Modest changes in cooling energy are realized between simulated cases. The greatest reduction in cooling energy was between two consecutive iteration cases with identical parameters. This example was between cases A-1 and A-2, where cooling energy reduced by 559 kWh (5%). This provided an example of a move from poor economizer control to improved control with an improvement in system efficiency. Proof of improvements shown between these cases are apparent by contrasting Figures 3.27 and 3.27.

Some heating energy was detected in August simulations. The presence of heating energy in August simulations is due primarily to a heating lock-out temperature that was too high to be ideal for summer use as well as a similar situation for heating plant control as explained previously. While other factors may be at play the fore-mentioned items are the only factors detected in this research. Based on the purpose and use of this facility as well as its location heating energy in August is of little or no consequence, thus it was ignored in the analysis.

It is suspected that further work into creating control sequences and an energy models which more carefully isolate the co-simulation to only cooling energy for purposes of understanding economizing would be helpful for identifying specific changes which would make further improvements to controller performance.

3.7 Conclusion

This research has demonstrated proof-of-concept for use of co-simulation as a tool to test and improve DDC controller programming. As part of this research custom logic was developed to test control schemes for both winter and summer operation of multiple constant-air-volume HVAC air handling units that would be compatible for use with an energy model. The control technique had to be adapted to be compatible with current EnergyPlus conventions for control of air loop HVAC components such as heating and cooling coil control. Instead of direct control of the fluid flow through the coil controller logic had to be modified to supply direct signals for SAT which EnergyPlus could use in simulation. This logic was developed and further modified and tuned based on results of co-simulations.

In particular two separate sets of cases were discussed for full month co-simulations run for January and August respectively. Adequate control of SAT to meet heating setpoints of various spaces was the focus in January cases, while control of economizer damper position as a means to improve cooling energy efficiency between cases. Two distinct but similar energy models of the actual facility approximated its energy behavior and one was employed primarily for August simulations whilst the other was used entirely for January simulations. This was necessary due to lack of capacity in the largest heating plant loop included in the original energy model. This prevented AHUs in previous test January simulations from reaching high enough supply air temperatures to reduce hours of unmet heating setpoint. January simulations using Model Q demonstrated improvements in time heating setpoint is met with a tradeoff of increases in heating energy. Case B-2 was a scenario where almost all zones were controlled reasonably well for meeting their setpoints, but in contrast with the

previous full month iteration, B-1, showed a significant increase in energy. Energy increased between these cases by 21 MWh, an increase of approximately 30%.

Sub-iterations between these milestone cases demonstrated changes to tuning parameters and control logic, results of which were analyzed against t_{HSPX} for the five control zones in order to determine custom changes for each of five control loops which would produce desired effects for an improved milestone case B-2. The problem of using EnergyPlus alone to efficiently model and adequately regulate SAT for multiple CAV AHUs each serving multiple zones via no reheat air terminals was examined in contrast the capability of co-simulation to assist with a challenging problem in energy modeling.

In August co-simulations economizer signals are improved between two similar sequentially iterative cases A-1 and A-2. In these cases identical parameters establishing the maximum SAT in heating mode T_{SAH} are employed and only changes to economizer logic are made to test effects of the changes. Results were compared and demonstrated improvement in economizer signals for all five AHUs as well as a 559 kWh (5%) reduction in cooling energy. Techniques described in this paper were used as a method to investigate the effectiveness of control schemes for efficiency in operation and energy use. Once a co-simulation model is completed, controller logic may be tested in a more automated fashion than is possible in the field. A programmer may input sequences into a controller that may be tested using an appropriate energy model. Instead of having to wait days, weeks or longer to see how changes in programming alter mechanical performance, effects for lengthy periods may be simulated in relatively short timeframes. In its current form, the technology allows the user to view simulation output as it progresses. If there is a significant problem with a parameter or programming it is not necessary to allow the simulation to run to completion before making an iterative change. Thus it is possible to commission certain aspects of controller function in a more automated fashion using co-simulation.

This technology is still in its infancy, but results from this and previous testing indicate strong potential. In its current prototype form, this technology has certain limitations.

Establishing communication with an energy model requires a significant effort from the user. It is fathomable that a middleware such as BCVTB may be more fully integrated into an energy modeling software package to automate the process of establishing full loop communication with an energy model. Application of optimization algorithms to make more appropriate selection for parameters may further automate the process.

Energy modeling software could also be better adapted for hardware in the loop co-simulation by more accurately simulating actual sequences and functions of mechanical systems. In this manner systems modeled may be controlled in a fashion more representative of physical reality. Examples of this are found in air handling unit function. From this research, for example, it was discovered that in its current form EnergyPlus does not allow the user to model control of supply air temperature by means of controlling coil valve positions. With continued improvements to the software involved, validation and improvement of controller programming may be further automated.

CHAPTER 4

SUMMARY AND CONCLUSIONS

This thesis has presented two studies which investigated use of BCVTB for two primary purposes. Chapter 2, “OPTIMIZATION OF SUPPLY AIR TEMPERATURE USING CONTROLLER-IN-THE-LOOP CO-SIMULATION,” examined BCVTB as a tool for pre-commissioning building automation and control systems. Specifically, this chapter focused on the feasibility of the Building Controls Virtual Testbed for commissioning air handler controllers. Chapter 3, “DYNAMIC PROGRAMMING AND VIRTUAL COMMISSIONING OF BUILDING CONTROL SYSTEMS THROUGH CO-SIMULATION” focused on the use of BCVTB to assist in programming and testing building controls.

The first item this research demonstrated is proof-of-concept for virtual commissioning of AHU controllers. In [28], control of economizer function in an energy co-simulation is demonstrated. Additional testing using the same energy model was performed to demonstrate control of AHU supply air temperature and presented in this thesis. Each of these cases are examples of how co-simulation can provide additional capabilities to energy modeling specific to analysis of actual performance of control hardware. Modeling packages such as EnergyPlus include energy management features which allow for custom control routines. Thus modeling various control capabilities with these features is possible without using co-simulation. In some cases these features may be sufficient to demonstrate energy savings without the hassle of developing simulations involving actual control hardware. Even still, these features must be integrated by use of advanced techniques.

The process of using of EnergyPlus for modeling energy management systems (EMS) is described in [15]. Additional programming is required to perform this variation of advanced energy analysis in EnergyPlus simulations. This capability requires use of additional programming using a simplified programming language called the EnergyPlus Runtime Language (Erl). Programs developed using Erl are referenced by the EnergyPlus input data file (.idf) and the Erl program interacts with the simulation as it progresses. BCVTB in-

teracts with EnergyPlus in a similar fashion except energy management schemes are 100% externally applied to the simulation instead of from within the inherent framework of EnergyPlus. Theoretically, it should not matter whether a specific change to simulated behavior is dictated within or without of the inherent framework. Simulation results would in theory be unaffected by the method of implementing an identical control measure, whether it is through EnergyPlus EMS protocol or a parameter communicated from a BACnet controller via BCVTB. However, validating this hypothesis would have to be a topic of subsequent research.

A focus of future development in energy modeling software could be the addition of streamlined integration features for a co-simulation platform like BCVTB or capabilities for more simplified integration of EMS measures. Regardless of which of these approaches seems to warrant accommodations in terms of future application development, there are a two specific improvements which seem relevant for both. These improvements are 1.), making the process of implementing control measures more automated; And 2.), ensuring energy modeling applications allow for external control for variables common to physical systems which are likely to be directly controlled by DDC equipment.

More streamlined approaches should be developed for advanced control measures in energy modeling applications. Evidence that this endeavor would be worthwhile is outlined in results and conclusion sections included throughout this paper. This research identified areas for improved control using co-simulation and demonstrated the ability to predict energy benefits of implementing these measures. Furthermore, the techniques described for pre-commissioning building controls in this paper may be applied in a relatively short timeframe. Commissioning and optimizing equipment historically has been a process conducted over the first couple of years of a building's life. An annual energy co-simulation can be run to completion anywhere between one and nine days. This is a substantial improvement over a couple or few years worth of time.

In some cases it was not possible to control a particular parameter using BCVTB. This

was due to a deficiency of the energy modeling software in terms of its ability to allow for control of a particular variable. One example was the inability to model control of air handling unit heating and cooling coil volumetric flow rate to simulate control of coil valve positions. A second example was the inability to simulate control of fan speed for the air handling units using an external interface.

Advantages of using BCVTB in lieu of built in EMS capability will primarily depend on the user's intent. For instance, a DDC programmer wishing to test the result of modifying a particular control parameter, may benefit from an ability to plug existing control sequences residing on test controllers into an EnergyPlus simulation using co-simulation techniques. This would likely be the case if the process of integrating real controllers into an energy simulation were greatly simplified from current integration requirements. Also, energy modeling is not likely included among specialties typical for DDC programmers. Due to the level of specialization involved in DDC programming, programmers would not likely have the time required to build and test energy models, let alone integrate their controls into these models using rather complex techniques. For an energy modeling expert approached by an architect, engineer, owner, or building operator wanting to know the effect of certain changes in equipment operation on energy consumption, perhaps the EnergyPlus EMS conventions would be the correct approach. As part of a collaborative effort, however, an integrated approach for commissioning equipment which includes several professionals may be possible.

Assuming that pre-commissioning efforts are best suited to an integrated effort involving the gamut of building professionals, it seems that development of more automated integration capabilities for energy co-simulation would be particularly useful. This is because currently buildings are controlled by real building automation equipment and not by energy models. In Chapter 3, the ability to make changes to DDC programming and test these changes was investigated. Through the research described in Chapter 3, the ability to test programming changes and predict potential benefits was demonstrated. Thus using co-simulation frameworks which allow for controller-in-the-loop energy simulation appear

better suited than EnergyPlus EMS conventions for translating simulated control changes into actual implementations. Thus future software developments aiming towards a more automated energy co-simulation framework in an energy modeling application would be a worthwhile endeavor. Finally, implementing actual control changes based on findings in this work or subsequent studies are topics for future research and may contribute to the case for software improvements which have been proposed in this section.

REFERENCES

- [1] Alerton. *Programmer's guide and reference: BACtalk Systems*. Novar Controls Corporation (2006).
- [2] ASHRAE. *ASHRAE Guideline 14 Measurement of Energy And Demand Savings*. American Society of Heating, Refrigerating and Air-Conditioning Engineers, Inc. (2002).
- [3] Bing Dong, Zheng O'Neil, and Zehengwei Li. A BIM-enabled information infrastructure for building energy fault detection and diagnostics. *Automation in Construction*, 44:197–211, 2014.
- [4] Irene Hafner, Matthias Rossler, Bernhard Heinzl, Andreas Korner, Felix Breitenecker, Michael Landsiedl, and Wolfgang Kastner. Using BCVTB for co-simulation between Dymola and MATLAB for multi-domain investigations of production plants. *Proceedings of the Ninth international Modelica conference, Munich, Germany*, pages 557–564, 2012.
- [5] Lincoln C. Harmer and Gregor P. Henze. Using calibrated energy models for building commissioning and load prediction. *Energy and Buildings*, 92:204–215, 2015.
- [6] Phillip Haves and Peng Xu. The building controls virtual test bed - a simulation environment for developing and testing control algorithms, strategies and systems. *IBPSA Conference Proceedings: Building Simulation*, pages 1440–1446, 2007.
- [7] Mark Hydeman, Steven T. Taylor, and Brent Eubanks. Control sequences & controller programming. *ASHRAE*, March:58–62, 2015.
- [8] Hangfeng Ji, Qiong Zhao, Xiaodong Wang, and Quanming Sum. Automatic assisted calibration tool for coupling building automation system trend data with commissioning. *Automation in Construction*, 61:124–133, 2016.
- [9] Bohdan T. Kulakowski, John F. Gardner, and J. Lowen Shearer. *Dynamic modeling and control of engineering systems*. Cambridge University Press, third edition, 2007.

- [10] S. Leal, G. Hauer, and F. Judex. A software architecture for simulation support in building automation. *Energy and Buildings*, 4:320–335, 2014.
- [11] Yuezhong Liu, YiChun Huang, and Rudi Stouffs. Using a data-driven approach to support the design of energy-efficient buildings. *Journal of Information Technology in Construction*, 20:80–96, 2015.
- [12] Thierry Nouidui. BACnet and analog-digital interfaces of the Building Controls Virtual Testbed. *Lawrence Berkeley National Laboratory*, LBNL5446E:1–11, 2013.
- [13] U.S. Department of Energy. *EnergyPlus Engineering Reference*. Lawrence Berkeley National Laboratory (2014).
- [14] U.S. Department of Energy. *EnergyPlus Input Output Reference*. Lawrence Berkeley National Laboratory (2014).
- [15] U.S. Department of Energy. *Using EnergyPlus for Energy Management System EMS Application Guide*. Lawrence Berkeley National Laboratory (2014).
- [16] Xiufeng Pang, Michael Wetter, Prajesh Bhattacharya, and Philip Haves. A framework for simulation-based real-time whole building performance assessment. *Building and Environment*, 54:100–108, 2012.
- [17] Aleksander Preglej, Jakob Rehrl, Daniel Schwingshackl, Igor Steiner, Martin Horn, and Igor Skrjanc. Energy-efficient fuzzy model-based multivariable predictive control of an hvac system. *Energy and Buildings*, 82:520–5333, 2014.
- [18] Guang Qu and Mo Zaheeruddin. Online H_∞ adaptive tuning of PI controllers for discharge air temperature system. *Energy Conversion and Management*, 51:1179–1195, 2010.
- [19] Eric Shen, Jia Hu, and Maulin Patel. Energy and visual comfort analysis of lighting and daylight control strategies. *Building and Environment*, 78:1440–1446, 2014.

- [20] Servet Soyguder, Mehmet Karakose, and Hasan Alli. Design and simulation of self-tuning PID-type fuzzy adaptive control for an expert hvac system. *Expert systems with applications*, 36:4566–4573, 2009.
- [21] Gang Wang and Li Song. Air handling unit supply air temperature optimal control during economizing cycles. *Energy and Buildings*, 49:310–316, 2013.
- [22] Ling Wang, Steve Greenberg, John Fiegel, Alma Rubalcava, Shankar Earni, Xiufeng Pang, Rongxin Yin, Spencer Woodworth, and Jorge Hernandez-Maldonado. Monitoring-based HVAC commissioning of an existing office building for energy efficiency. *Applied Energy*, 102:1382–1390, 2013.
- [23] Ling Wang, Haoqi Ni, Ruixin Yang, Panos M. Pardalos, Li Jia, and Minrui Fei. Intelligent virtual reference feedback tuning and its application to heat treatment furnace control. *Engineering applications of artificial intelligence*, 46:1–9, 2015.
- [24] Michael Wetter. Co-simulation of building energy and control systems with the building controls virtual test bed. *Building Performance Simulation*, 4(3):185–203, 2011.
- [25] Michael Wetter and Thierry Noudui. *Building Controls Virtual Testbed User Manual*. Lawrence Berkeley National Laboratory (2015).
- [26] Michael Wetter and Jonathan Wright. Comparison of generalized pattern search and a genetic algorithm optimization method. *Proc. of the 8th IBPSA Conference*, 3(Eindhoven, Netherlands):1401–1408, 2003.
- [27] Michael Wetter and Jonathan Wright. Optimization of an hvac system with a strength multi-objective particle-swarm algorithm. *Energy*, 36:5935–5943, 2011.
- [28] Damon Woods, Tyler Noble, Brad Acker, Ralph Budwig, and Kevin Van Den Wymenlenberg. *Economizer optimization through co-simulation*, 2016. In Progress.